Correlations for the Viscosity and Thermal Conductivity of Tetrahydrofuran

Sofia Sotiriadou[1], Eleftheria Ntonti[1], Marc J. Assael[1,a], Konstantinos D Antoniadis[1], and Marcia L. Huber[2]

[1] *Laboratory of Thermophysical Properties and Environmental Processes, Chemical Engineering Department, Aristotle University, Thessaloniki 54636, Greece*

[2] *Applied Chemicals and Materials Division, National Institute of Standards and Technology, 325 Broadway, Boulder, CO 80305, USA*

We present hybrid predictive-correlative engineering correlations for the calculation of the viscosity and thermal conductivity of tetrahydrofuran (THF) in the fluid phase. They incorporate critically evaluated experimental data where available, and predictive methods in regions where there are no data and can be applied over the gas, liquid, and supercritical phases. The viscosity correlation is validated from 195 K to 353 K, and up to 30 MPa pressure, while the thermal conductivity is validated in the temperature range 174 K to 332 K, and up to 110 MPa pressure. Both correlations are designed to be used with a recently published equation of state that extends from the triple point to 550 K, at pressures up to 600 MPa. The estimated uncertainty (at a 95% confidence level) for the viscosity is 10% for the low-density gas (up to atmospheric pressure), and 6% for the liquid at temperatures up to 353 K and pressures up to 30 MPa. For thermal conductivity, the expanded uncertainty is estimated to be 15% for the low-density gas, and 2% for the liquid phase from the triple-point temperature to 330 K at pressures up to 15 MPa, rising to 4% at 110 MPa. Due to the extremely limited data available, these correlations should be considered preliminary until further experimental data become available.

Key words: tetrahydrofuran; thermal conductivity; transport properties; viscosity.

[a)] Author to whom correspondence should be addressed (marc.assael@gmail.com)

1 Introduction

Tetrahydrofuran (THF) also known as oxolane (IUPAC name), or 1,4-epoxybutane, has the molecular formula of C_4H_8O. THF has a primary use as a solvent in organic synthesis and chromatographic analysis, and is an intermediate of nylon-6,6. It is also used as an intermediate for synthetic pesticides (e.g. fenbutatin), it is directly employed in the production of synthetic fibers, resins, and rubbers, as well as a solvent for many polymeric materials [1]. Furthermore, THF is widely employed in surface coatings, anticorrosion coatings, and printing inks. In the pharmaceutical industry, THF is used for the synthesis of carbetapentane, rifamycin, progesterone, and some hormone drugs [1]. Regardless of its wide range of applications, there is currently no reference correlation for the viscosity, nor the thermal conductivity of THF, probably attributed to the fact that an equation of state for THF has only just now been published [2].

In a series of papers published over the last ten years, we reported new reference correlations over extended temperature and pressure ranges for the viscosity of some simple fluids [3-6], hydrocarbons [7-14], alcohols [15-18], and some refrigerants [19-23]. In the case of the thermal conductivity, we also reported new reference correlations over extended temperature and pressure ranges, for some simple fluids [24-30], hydrocarbons [9, 10, 14, 31-38], alcohols [39, 40], and some refrigerants [21, 22, 41, 42]. In this paper, the methodology adopted in the aforementioned papers is extended to developing new correlations for the viscosity and thermal conductivity of THF. Therefore, the goal of this work is to critically assess the available literature data, and provide wide-ranging correlations for the viscosity and thermal conductivity of THF that are valid over gas, liquid, and supercritical states, and incorporate densities provided by the recently published equation of state of Fiedler et al. [2].

The analysis we use is based on the best available experimental data. A prerequisite to the analysis is a critical assessment of the experimental data. Here we define two categories of experimental data: primary data, employed in the development of the correlation, and secondary data, used simply for comparison purposes. According to the recommendation adopted by the Subcommittee on Transport Properties (now known as The International Association for Transport Properties) of the International Union of Pure and Applied Chemistry, the primary data are identified by a well-established set of criteria [43] These criteria have been successfully employed to establish standard reference values for the viscosity and thermal conductivity of fluids over wide ranges of conditions, with uncertainties in the range of 1%. However, in many cases, such a narrow definition unacceptably limits the range of the data representation. Consequently, within the primary data set, it is also necessary to include results that extend over a wide range of conditions, albeit with a poorer accuracy, provided they are consistent with other more accurate data or with theory. In all cases, the accuracy claimed for the final recommended data must reflect the estimated uncertainty in the primary information.

The development of the correlation requires densities; Fiedler et al. [2] has recently published an accurate, wide-ranging Helmholtz-energy equation of state valid from the triple point up to 550 K and 600 MPa, with an uncertainty of 0.015 % (95% confidence level) in density. We use the Fiedler et al. [2] EOS for all thermodynamic properties and also adopt their values for the critical point and triple

point. The critical temperature, T_c, and the critical density, ρ_c, are 540.20 K and 317.265168 kg·m^{-3}, respectively [2] and the triple-point temperature is 164.76 K [2].

2 The viscosity correlation

The viscosity η can be expressed [3-13, 15-23] as the sum of four independent contributions, as

$$\eta(\rho,T) = \eta_0(T) + \eta_1(T)\rho + \Delta\eta(\rho,T) + \Delta\eta_c(\rho,T), \quad (1)$$

where ρ is the molar density, T is the absolute temperature, and the first term, $\eta_0(T) = \eta(0,T)$, is the contribution to the viscosity in the dilute-gas limit, where only two-body molecular interactions occur. The linear-in-density term, $\eta_1(T)\,\rho$, known as the initial density dependence term, can be separately established with the development of the Rainwater-Friend theory [44-46] for the transport properties of moderately dense gases. The critical enhancement term, $\Delta\eta_c(\rho,T)$, arises from the long-range density fluctuations that occur in a fluid near its critical point, which contribute to divergence of the viscosity at the critical point. This term for viscosity is significant only in the region very near the critical point, as shown in Vesovic et al. [47] and Hendl et al. [48]. For CO_2, Vesovic et al. [47] showed that the enhancement contributes greater than 1% to the viscosity only in the small region bounded by $0.986 < T_r < 1.019$ and $0.642 < \rho_r < 1.283$ (where T_r and ρ_r denote the reduced temperature and density, T/T_c and ρ/ρ_c respectively). Since data close to the critical point are unavailable, $\Delta\eta_c(\rho,T)$ will be set to zero in Eq. 1 and not discussed further. Finally, the term $\Delta\eta(\rho,T)$, the residual term, represents the contribution of all other effects to the viscosity of the fluid at elevated densities including many-body collisions, molecular-velocity correlations, and collisional transfer.

The identification of these four separate contributions to the viscosity and to transport properties in general is useful because it is possible, to some extent, to treat $\eta_0(T)$ and $\eta_1(T)$ theoretically. In addition, it is often possible to derive information about both $\eta_0(T)$ and $\eta_1(T)$ from experiment. In contrast, there is little theoretical guidance concerning the residual contribution, $\Delta\eta(\rho,T)$, and therefore its evaluation is based entirely on an empirical equation obtained by fitting experimental data.

Table 1 Viscosity measurements of THF

Investigators/reference	Publ. Year	Technique employed[a]	Purity (%)	Uncer-tainty (%)	No. of data	Temperature range (K)	Pressure range (MPa)
Primary data							
Al Tuwaim et al. [49]	2018	CAP	99.0	0.25	3	298-308	0.1
Muhamed et al. [50]	2017	CAP	99.0	0.25	5	303-323	0.1
Droliya and Nain [51]	2017	CAP	99.5	1.0	6	293-318	0.1
Chen et al. [52]	2015	RBal	99.9	1.0	7	293-323	0.1
Zivkovic et al. [53]	2014	CAP	99.0	0.8[b]	8	288-323	0.1
Knezevic-Stevanoivic et al. [54]	2014	CAP	99.5	0.8[b]	8	288-323	0.1
Sinha et al. [55]	2013	CAP	99.5	0.7	3	298-318	0.1
Rathnam et al. [56]	2013	CAP	99.6	1.0	3	303-313	0.1
Wankhede et al. [57]	2010	CAP	LabP	0.65	3	288-308	0.1
Ku et al. [58]	2008	RBal	99.5	1.3	3	298-308	0.1
Giner et al. [59]	2006	CAP	99.5	0.5	2	298, 313	0.1
Nayak et al. [60]	2004	CAP	99.7	0.25	3	303-323	0.1
Nayak et al. [61]	2003	CAP	99.7	0.25	3	298-308	0.1
Postigo et al. [62]	2003	CAP	99.8	0.7	3	283-313	0.1
Mariano et al. [63]	2000	CAP	99.5	1.0	3	283-313	0.1
Muhuri et al. [64]	1996	CAP	LabP	0.2	3	298-318	0.1
Zhang and Liu [65]	1991	FCyl	99.5	2.0	28	298-338	0.1-30
Oswal [66]	1988	CAP	99.5	0.7	2	303, 313	0.1
Oshmyansky et al. [67]	1986	CAP	99.0	2.0	2	298, 318	0.1
Metz and Glines [68]	1967	CAP	na	na	8	195-303	0.1
Carvajal et al. [69]	1965	CAP	na	1.0	10	203-298	0.1
Kuss [70]	1955	FBal	na	2.0	8	293-353	0.01-0.16
Secondary data							
Lin et al. [71]	2019	CAP	99.8	3.0	3	303-323	0.1
Hussain et al. [72]	2019	CAP	99.6	4.5	1	303	0.1
Duereh et al. [73]	2017	CAP	99.8	0.12	5	298-318	0.1
Patel et al. [74]	2015	CAP	99.5		4	298-313	0.1
Dubey and Kumar [75]	2014	CAP	99.0	0.08	1	298	0.1
Ekka and Roy [76]	2014	CAP	99.0	0.6	1	298	0.1
Elhami-Kalvanagh et al. [77]	2013	CAP	99.8	0.45	1	298	0.1
Zhu et al. [56]	2011	CAP	99.5	1.0	1	298	0.1
Fattahi and Iloukhani [78]	2010	CAP	99.0	0.05	3	288-308	0.1
Bhattacharjee and Roy [79]	2010	CAP	99.0	0.04	1	298	0.1
Rodnikova et al. [80]	2010	na	99.95	na	19	298	6.4-151
Al-Kandary et al. [81]	2009	RCyl	99.97	0.65[b]	1	298	0.1
Bandres et al. [82]	2009	CAP	99.5	na	1	298	0.1
Mohsen-Nia et al. [83]	2009	CAP	99.0	na	1	298	0.1
Oswal and Ijardar [84]	2009	CAP	99.5	0.05	1	303	0.1
Palani and Geetha [85]	2009	CAP	99.9	na	3	303-313	0.1
Parveen et al. [86]	2009	CAP	na	0.5	3	293-313	0.1
Marczak et al. [87]	2008	CAP	98.5	1.5	6	298-312	0.1
Nain [88]	2007	CAP	99.6	na	3	298-318	0.1
Zafarani-Moattar and Majdan-Cegincara [89]	2007	CAP	99.5	0.5	1	298	0.1
Sinha and Roy [90]	2007	CAP	99.5	0.05	1	298	0.1
Sinha and Roy [91]	2007	CAP	99.5	0.05	3	303-323	0.1
Singh [92]	2006	CAP	na	20	1	293	0.1
Parmar and Guleria [93]	2006	na	na	na	1	298	0.1
Tang et al. [94]	2006	CAP	99.0	0.6	1	298	0.1
Gupta et al. [95]	2006	CAP	na	na	3	293-313	0.1
Das and Roy [96]	2006	CAP	99.5	0.03	3	298-318	0.1
Choudhury et al. [97]	2005	CAP	na	0.05	3	299-298	0.1
Oswal et al. [98]	2005	CAP	99.8	0.05	1	303	0.1
Perez et al. [99]	2003	CAP	99.0	na	2	283-313	0.1
Baluga [100]	2002	CAP	99.95	0.1	1	313	0.1
Kinart et al. [101]	2002	na	na	na	3	293-303	0.1

Saleh et al. [102]	2001	CAP	99.5	0.14	5	303-323	0.1
Acevedo et al. [103]	2000	CAP	na	1.0	1	298	0.1
Kolosnitsyn et al. [104]	2000	na	99.5	na	1	303	0.1
Gascon et al. [105]	1999	CAP	99.5	na	2	298, 313	0.1
Chauhan et al. [106]	1999	na	na	na	1	298	0.1
Aminabhavi and Patil [107]	1998	CAP	99.2	0.03	3	298-308	0.1
Aralaguppi et al. [108]	1996	CAP	99.5	0.05	3	298-308	0.1
Bardavid et al. [109]	1996	CAP	LabP	1.1	1	298	0.1
Krishnaiah and Surendranath [110]	1996	CAP	LabP	0.1	1	303	0.1
Rodriguez et al. [111]	1996	CAP	99.5	na	1	298	0.1
Solimo and Gomez Marigliano [112]	1993	CAP	na	0.2	1	303	0.1
Cook et al. [113]	1992	DiAn	na	10.0	11	295	0.1-1885
Wencel and Czerepko [114]	1991	FBal	na	na	3	293-303	0.1
Ramkumar and Kudchadker [115]	1989	CAP	na	0.45	5	278-298	0.1
Matsuda et al. [116]	1986	na	na	na	1	303	0.1
Geerissen et al. [117]	1985	RBal	na	na	3	298-333	0.1
Ratkovics and Laszlone Parragi [118]	1984	na	na	na	2	293, 313	0.1
Gurevich et al. [119]	1982	CAP	na	na	7	273-333	0.006-0.08
Hayduk et al. [120]	1973	CAP	99.98	na	1	298	0.1
Holland and Smyth [121]	1955	na	na	na	3	274-313	0.1

[a] Cap, Capillary; DiAn; Diamond-Anvil cell; FBal, Falling Ball; FCyl, Falling Cylinder; LabP, Purified in author's Laboratory; RBal, Rolling Ball; RCyl, Rotating Cylinder.

[b] At the 95% confidence level

na not available.

Table 1 summarizes, to the best of our knowledge, the experimental measurements of the viscosity of THF reported in the literature. In relation to the selection of the primary data set of measurements at 0.1 MPa presented in Table 1, the same criteria adopted in our recent paper on the reference correlation of ethanol [16], were adopted. As already mentioned in the introduction, THF is extensively employed in experimental studies on volumetric and viscometric properties of binary and ternary mixtures, phase equilibria studies, or polymeric applications. In such studies, although the viscosity of pure THF is also measured, the emphasis is on the properties of the mixture, the solution, and the effect of the change in concentration. Hence, in recent literature, there is a very large number of papers that include a single measurement of the viscosity of THF at room temperature with inadequate assessments of uncertainty. Therefore, we did not include in the primary data set such articles with a single viscosity measurement at room temperature or near it. Furthermore, as water is the only liquid whose viscosity is known to an uncertainty as low as 0.17 % (at the 95 % confidence level) [43], all measurements in which the authors quote uncertainties of less than 0.2 % (e.g. 0.03 %!), characteristic of investigators that do not understand how to assess their measurement uncertainty, have been placed in the secondary data set. Since we are also interested in low-uncertainty measurements, we also did not consider for the primary data set measurements with quoted uncertainty larger than 2 %. In conclusion, for viscosity measurements at 0.1 MPa to be included in the primary data set,

1) must not be a single measurement at room temperature,
2) their quoted uncertainty must be between 0.2 % and 2 %, and
3) the purity of the sample and the technique employed must be stated.

Although not conforming to the above three criteria, we included three more sets to the primary data: the measurements of Kuss [70] as they extend to 353 K, as well as the measurements of Metz and Glines [68] and Carvajal et al. [69] as they were obtained at much lower temperatures such as 195 K and 203 K respectively. We note that the measurements of Marczak et al. [87] were not included in the primary data set as they show unexplainable deviations of up to 50 % higher than all other primary measurements.

As far as we know, there are only three sets of measurements performed under high pressures: Rodnikova et al. [80], Cook et al. [113], and Zhang and Liu [65]. The measurements of Rodnikova et al. [80] do not seem correct as extrapolation to 0.1 MPa produces a negative viscosity value. Furthermore, the viscosity values of ethylene glycol quoted in the same paper, are orders of magnitude away from known values [122]. Therefore, this set of measurements was not included in the primary data set. The measurements of Zhang and Liu [65] were performed in a falling-cylinder instrument with a 2 % uncertainty and were included in the primary data set. The third set of measurements, of Cook et al. [113] were performed with a 10 % uncertainty at 295.65 K, and extend to extremely high pressures (1885 MPa) exceeding the upper pressure limit (600 MPa) of the EOS of Fiedler et al. [2]. In addition, the data are presented only graphically, and the lowest pressure measurement is at 151 MPa. Preliminary attempts at correlating these data indicated that they are not consistent with of Zhang and Liu [65] and were therefore classified as secondary. Hence, the only set of measurements above atmospheric pressure are the data of Zhang and Liu [65].

Figures 1 and 2 show the ranges of the primary measurements outlined in Table 1, and the phase may be seen as well.

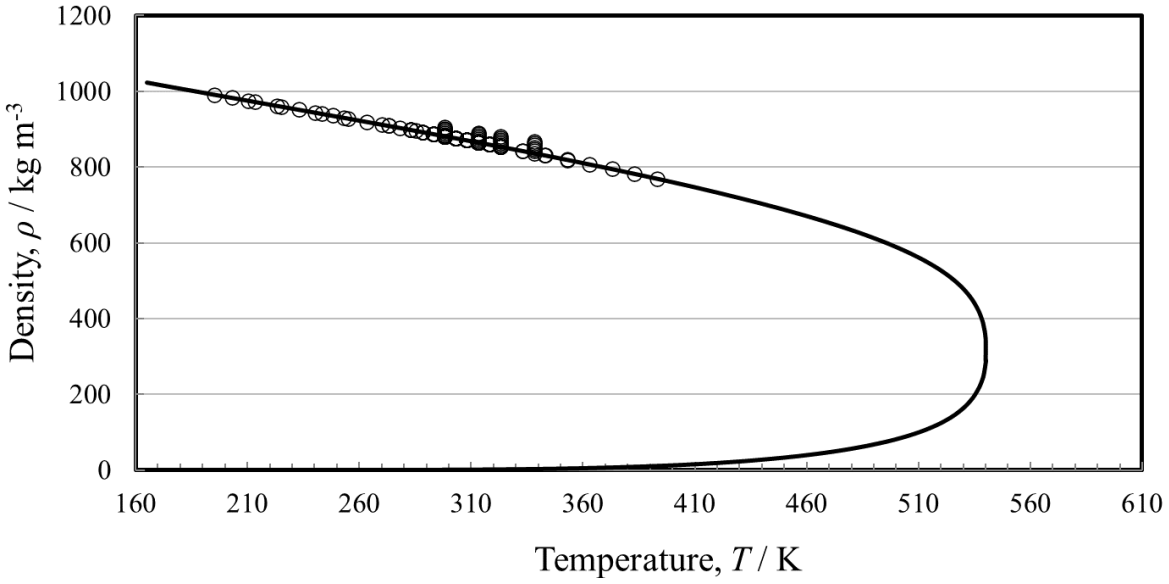

FIG. 1 Temperature-density ranges of the primary experimental viscosity data for THF, (—) saturation curve.

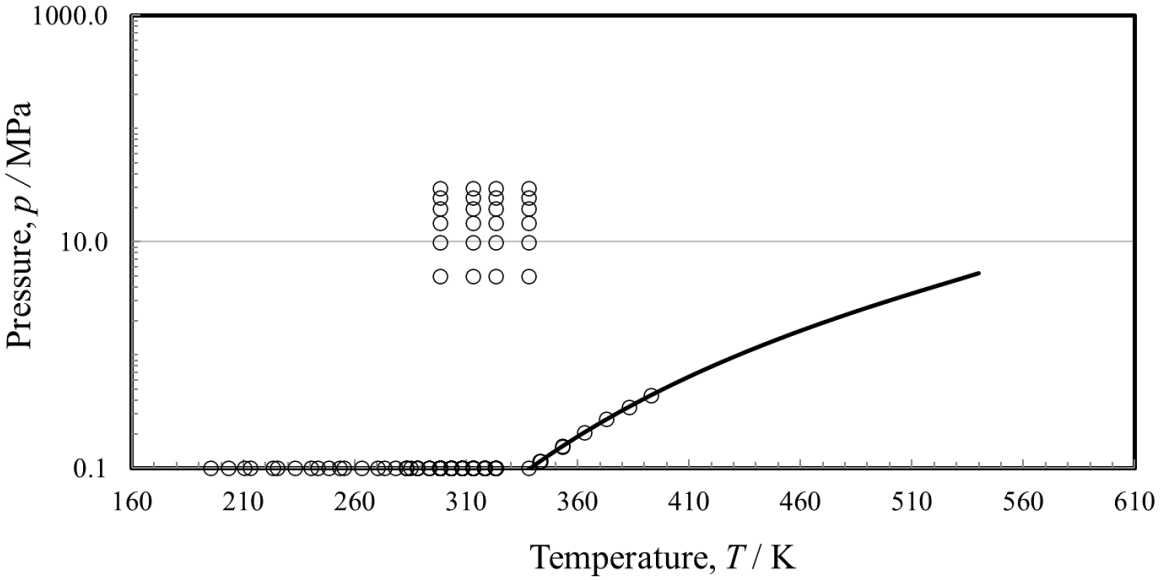

FIG. 2 Temperature-pressure ranges of the primary experimental viscosity data for THF, (—) saturation curve.

As shown in both figures, the data are extremely limited with a total lack of data in the vapor phase, as well as in the critical and supercritical ranges and only very limited data in the liquid above atmospheric pressure. This necessitates creating a hybrid model that combines predictive methods with correlation of experimental data when available.

2.1 The viscosity dilute-gas limit

The dilute-gas limit viscosity, $\eta_0(T)$ is a function only of temperature and can be analyzed independently of all other contributions in Eq. 1. According to the kinetic theory, the viscosity of a pure polyatomic gas may be related to an effective collision cross section, which contains all the dynamic and statistical information about the binary collision. For practical purposes, this relation is formally identical to that of monatomic gases and can be written as [123]

$$\eta_0(T) = 0.02669 \frac{\sqrt{MT}}{\sigma^2 \Omega^{(2,2)}} \tag{2}$$

where M (72.10572 g·mol^{-1}) is the molar mass, the collision diameter σ in nm is the smallest separation distance where the intermolecular potential function is equal to zero, T is the temperature in K, and the resulting viscosity is in μPa·s. $\Omega^{(2,2)}$ is a collision integral that depends upon the potential function.

Neufeld et al. [124] developed an empirical correlation for the $\Omega^{(2,2)}$ collision integral for the Lennard-Jones (12-6) potential, as a function of the dimensionless temperature $T^* = T/(\varepsilon/k_B)$ (where k_B is Boltzmann's constant and ε is the Lennard-Jones energy parameter), as

$$\Omega^{(2,2)}(T^*) = 1.16145(T^*)^{-0.14874} + 0.52487\,\mathrm{e}^{-0.7732T^*} + 2.16178\,\mathrm{e}^{-2.43787T^*} - 6.435\times10^{-4}(T^*)^{0.14874}\sin\left[18.0323(T^*)^{-0.7683} - 7.27371\right] \quad . \tag{3}$$

Equations 2 and 3 form a consistent scheme for the calculation of the dilute-gas limit viscosity as a function of the temperature, the only unknowns being the parameters σ and ε. Since there are no vapor measurements of THF, we employed the estimation method of Chung et al. [125] for these parameters and the values obtained are shown in Table 2. Figure 3 shows the gas-phase low-pressure data calculated using Eqs. 2 and 3.

For ease of use in calculations, η_0 values calculated from Eqs. 2 and 3 over the temperature range 165 to 1500 K were fitted using a commercial program ([126]) to a rational polynomial :

$$\eta_0(T_\mathrm{r}) = \frac{0.686304 + 11.1787T_\mathrm{r} - 0.638708T_\mathrm{r}^2 + 13.5305T_\mathrm{r}^3 - 0.739109T_\mathrm{r}^4}{0.983801 - 0.402682T_\mathrm{r} + T_\mathrm{r}^2}, \tag{4}$$

where the units for η_0 are μPa·s, and the reduced temperature is $T_\mathrm{r} = (T/T_\mathrm{c})$. Eq. 4 reproduces the values calculated by Eqs. 2 and 3 to within 0.07 % up to 1500 K, and thus it will be employed hereafter. The estimated uncertainty of the dilute-gas correlation, Eq. 4, is 10%.

Table 2 Parameters for THF

Parameters	
M (g·mol^{-1})	72.10572
T_c (K)	540.2
ρ_c (kg·m^{-3})	317.265168
ε/k_B (K)	428.92
σ (nm)	0.494

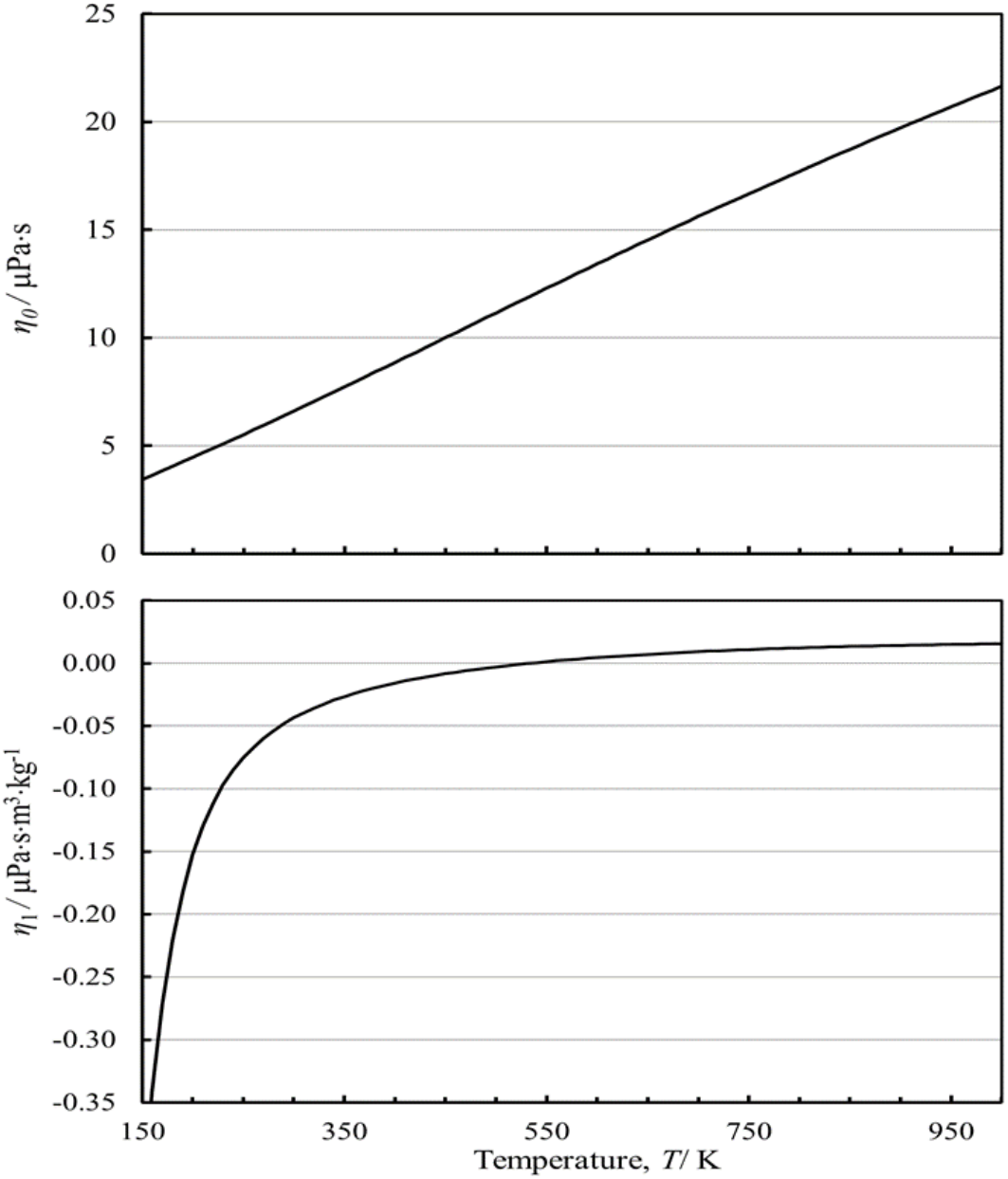

FIG. 3 Above: Dilute-gas viscosity, η_0, as a function of the temperature. Below: Initial-density dependence viscosity coefficient, η_1.

2.2 The initial-density dependence viscosity term

The temperature dependence of the linear-in-density coefficient of the viscosity $\eta_1(T)$ in Eq. 1 is very large at subcritical temperatures and must be considered to obtain an accurate representation of the behavior of the viscosity in the vapor phase. It changes sign from positive to negative as the temperature decreases. Therefore, the viscosity along an isotherm should first decrease in the vapor phase and subsequently increase with increasing density [123]. Vogel *et al.*[127] have shown that fluids exhibit the same general behavior of the initial density dependence of viscosity, which can also be expressed by means of the second viscosity virial coefficient $B_\eta(T)$ in $m^3 \cdot kg^{-1}$, as

$$B_\eta(T) = \frac{\eta_1(T)}{\eta_0(T)}. \tag{5}$$

The second viscosity virial coefficient can be obtained according to the theory of Rainwater and Friend [44, 45] as a function of a reduced second viscosity virial coefficient, $B_\eta^*(T^*)$, as

$$B_\eta^*(T^*) = \frac{B_\eta(T)}{N_A \sigma^3}, \tag{6}$$

where [123]

$$B_\eta^*(T^*) = \sum_{i=0}^{6} d_i \left(T^*\right)^{-0.25i} + d_7 \left(T^*\right)^{-2.5} + d_8 \left(T^*\right)^{-5.5}. \tag{7}$$

In the above equations, N_A is the Avogadro constant. The coefficients d_i from ref. [123] are given in Table 3. Fig. 3 shows the initial-density dependence viscosity term as a function of the temperature.

Table 3 Coefficients for Eqs. 7 and 8.

i	d_i (-) - Eq. 7 [123]	f_i (-) - Eq. 8
0	-0.195728810×10^2	-0.78446298500 ×10^1
1	0.219739990×10^3	0.11030973567×10^2
2	-0.101532260×10^4	-0.15885914893×10^1
3	0.247101251×10^4	0.96193104071×10^2
4	-0.337517170×10^4	0.33039653165×10^2
5	0.249165970×10^4	0.11207063543×10^2
6	-0.787260860×10^3	-0.66931945420×10^1
7	0.140854550×10^2	
8	-0.346641580×10^0	

2.3 The viscosity residual term

The residual viscosity term $\Delta\eta(\rho,T)$, represents the contribution of all other effects to the viscosity of the fluid at elevated densities including many-body collisions, molecular-velocity correlations, and collisional transfer. Because there is little theoretical guidance concerning this term, its evaluation here is based entirely on experimentally obtained data.

The procedure adopted during this analysis used symbolic regression software [128] to fit all the primary data to the residual viscosity. Symbolic regression is a type of genetic programming that allows the exploration of arbitrary functional forms to regress data. The functional form is obtained by use of a set of operators, parameters, and variables as building blocks. In the present work we restricted the operators to the set (+,–,*,/) and the operands (constant, T_r, ρ_r), with $T_r = T/T_c$ and $\rho_r = \rho/\rho_c$. In addition,

we adopted a form suggested from the hard-sphere model employed by Assael *et al.* [129] $\Delta\eta(\rho_r,T_r)=(\rho_r^{2/3}T_r^{1/2})F(\rho_r,T_r)$, where the symbolic regression method was used to determine the functional form for $F(\rho_r,T_r)$. For this task, the dilute-gas limit and the initial density dependence terms were calculated for each experimental point (employing Eqs. 4 - 7) and subtracted from the experimental viscosity to obtain the residual term. The final equation obtained was

$$\Delta\eta(\rho,T)=\left(\rho_r^{2/3}T_r^{1/2}\right)\left\{f_0+f_1T_r+f_2\rho_r+\frac{f_3+f_4T_r}{f_5+f_6\rho_r+\rho_r^2}\right\}. \tag{8}$$

The coefficients f_i are given in Table 3.

2.4 Comparison with data

The final correlation consists of Eq. 1, and Eqs. 4 - 8 with the critical enhancement term set to zero. Table 4 summarizes comparisons of the primary data with the correlation, and Table 5 gives comparisons for the secondary data. We define the percent deviation as PCTDEV = $100(\eta_{exp}-\eta_{fit})/\eta_{fit}$, where η_{exp} is the experimental value of the viscosity and η_{fit} is the value calculated from the correlation. The average absolute percent deviation (AAD) is found with the expression AAD = $(\sum \left| \text{PCTDEV} \right|)/n$, where the summation is over all n points, the bias percent is found with the expression BIAS = $(\sum \text{PCTDEV})/n$.

The average absolute percentage deviation of the fit for the primary data is 2.43 %, with a bias of 1.25%, while the estimated uncertainty of the correlation in the temperature range 195 to 353 K and up to 30 MPa in the liquid phase is 6.0 % (at the 95% confidence level). Due to the omission of a critical enhancement term, in the near vicinity of the critical point the uncertainty can be larger.

Table 4 Evaluation of THF viscosity correlation for the primary data.

Investigators/reference	Year Publ.	AAD (%)	BIAS (%)
Al Tuwaim et al. [49]	2018	0.37	0.00
Muhamed et al. [50]	2017	3.54	2.76
Droliya and Nain [51]	2017	1.69	0.66
Chen et al. [52]	2015	3.88	3.88
Zivkovic et al. [53]	2014	4.47	4.47
Knezevic-Stevanoivic et al. [54]	2014	6.16	6.16
Sinha et al. [55]	2013	1.96	1.96
Rathnam et al. [56]	2013	1.59	0.38
Wankhede et al. [57]	2010	1.09	0.33
Ku et al. [58]	2008	2.28	2.28
Giner et al. [59]	2006	0.24	0.24
Nayak et al. [60]	2004	3.06	3.06
Nayak et al. [61]	2003	5.07	5.07
Postigo et al. [62]	2003	1.28	-0.62
Mariano et al. [63]	2000	1.22	-0.64
Muhuri et al. [64]	1996	1.95	1.95
Zhang and Liu [65]	1991	2.52	-0.15
Oswal [66]	1988	1.41	1.41
Oshmyansky et al. [67]	1986	1.39	-1.05
Metz and Glines [68]	1967	1.30	-1.30
Carvajal et al. [69]	1965	0.66	0.46
Kuss [70]	1955	1.07	-0.97
Total		**2.43**	**1.25**

Figure 4 shows the relative deviations of the primary viscosity data of THF from the values calculated by Eqs. 1, 4 - 8, as a function of temperature, while Figs. 5 and 6 show the same deviations but as a function of the pressure and the density.

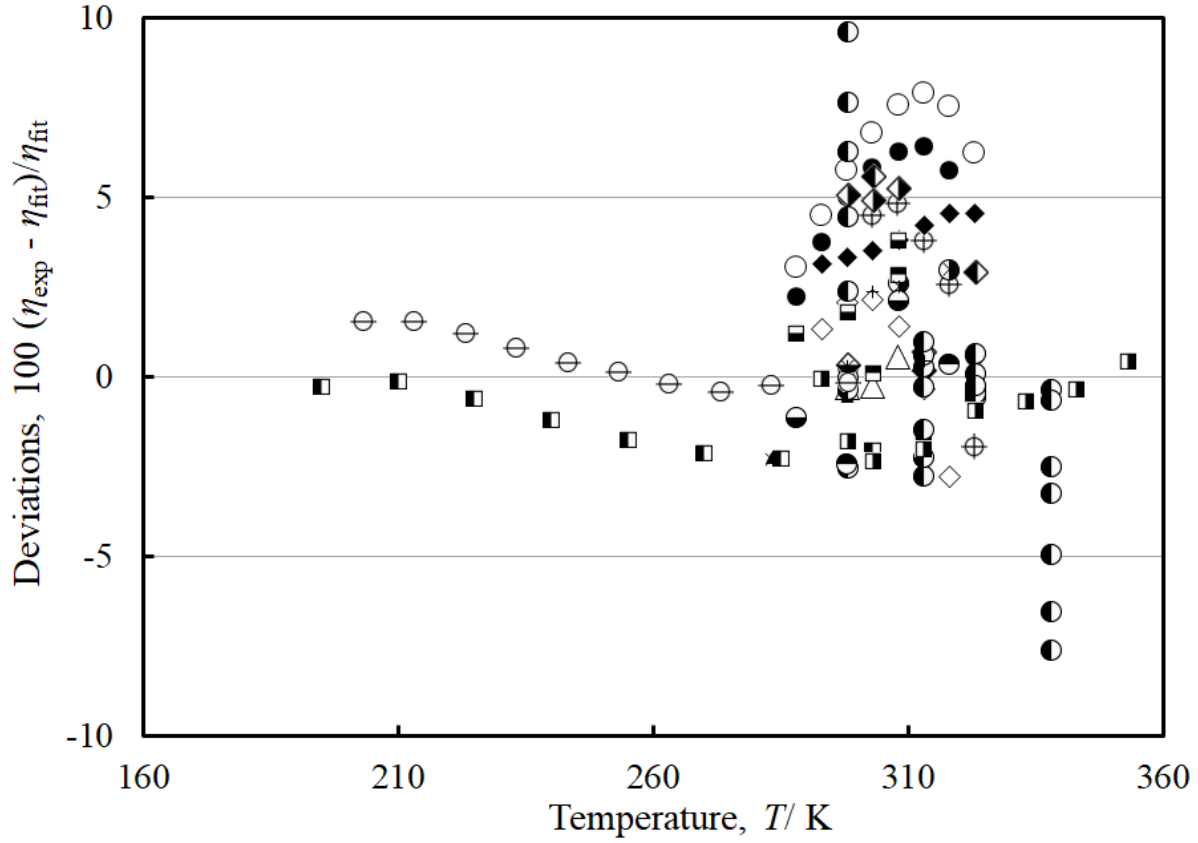

FIG. 4 Relative deviations of the viscosity of the primary experimental data of THF from the values calculated by the present scheme, Eqs. 1, 4-8, as a function of the temperature. Al Tuwaim et al. [49] (△), Muhamed et al. [50] (⊕), Droliya and Nain [51] (◇), Chen et al. [52] (◆), Zivkovic et al. [53] (●), Knezevic-Stevanoivic et al. [54] (○), Sinha et al. [55] (◑), Rathnam et al. [56] (⬒), Wankhede et al. [57] (◒), Ku et al. [58] (⬓), Giner et al. [59] (⬙), Nayak et al. [60] (⬖), Nayak et al. [61] (⬗), Postigo et al. [62] (▲), Mariano et al. [63] (x), Muhuri et al. [64] (✶), Zhang and Liu [65] (◐), Oswal [66] (+), Oshmyansky et al. [67] (◓), Metz and Glines [68] (◧), Carvajal et al. [69] (⊖), Kuss [70] (◨).

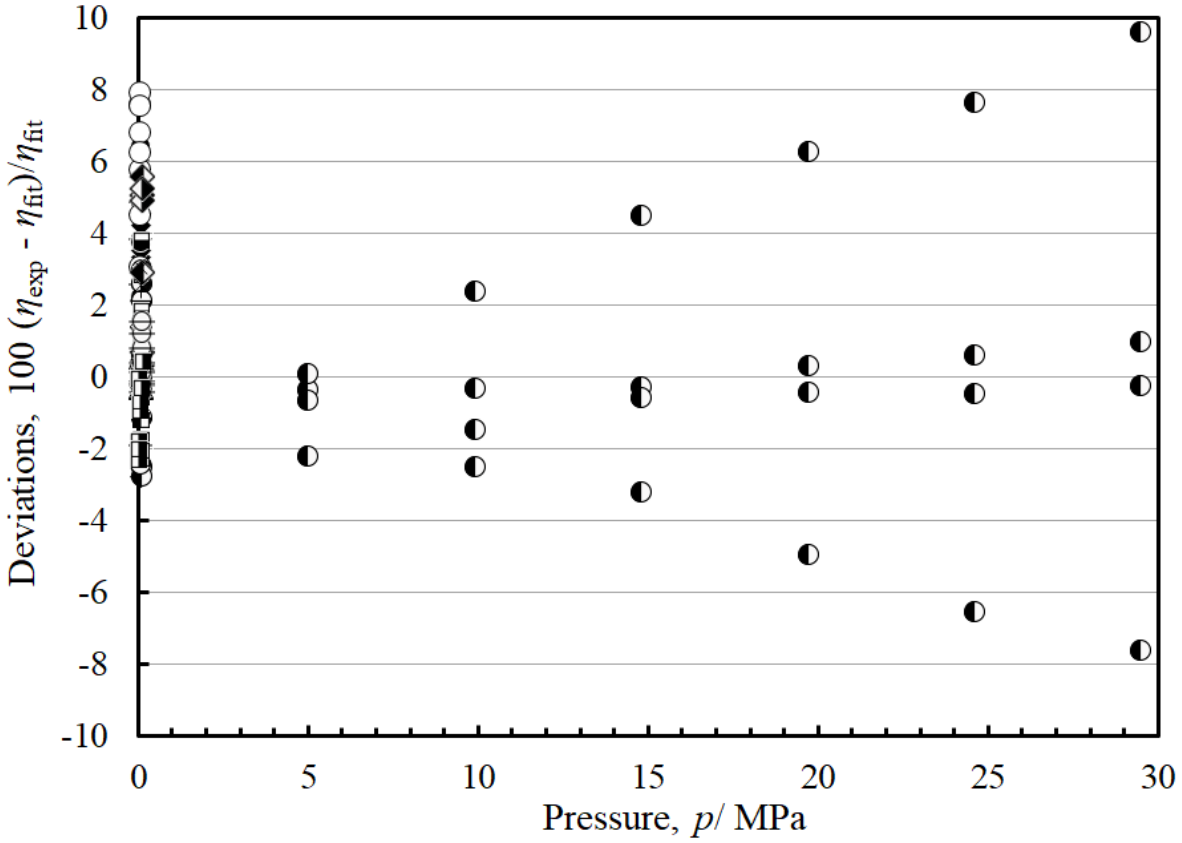

FIG. 5 Relative deviations of the viscosity of primary experimental data of THF from the values calculated by the present scheme, Eqs. 1, 4-8, as a function of pressure. Al Tuwaim et al. [49] (△), Muhamed et al. [50] (⊕), Droliya and Nain [51] (◇), Chen et al. [52] (◆), Zivkovic et al. [53] (●), Knezevic-Stevanoivic et al. [54] (○), Sinha et al. [55] (◑), Rathnam et al. [56] (⬒), Wankhede et al. [57] (◒), Ku et al. [58] (⬓), Giner et al. [59] (⬙), Nayak et al. [60] (⬖), Nayak et al. [61] (⬗), Postigo et al. [62] (▲), Mariano et al. [63] (x), Muhuri et al. [64] (✶), Zhang and Liu [65] (◐), Oswal [66] (+), Oshmyansky et al. [67] (◓), Metz and Glines [68] (◧), Carvajal et al. [69] (⊖), Kuss [70] (◨).

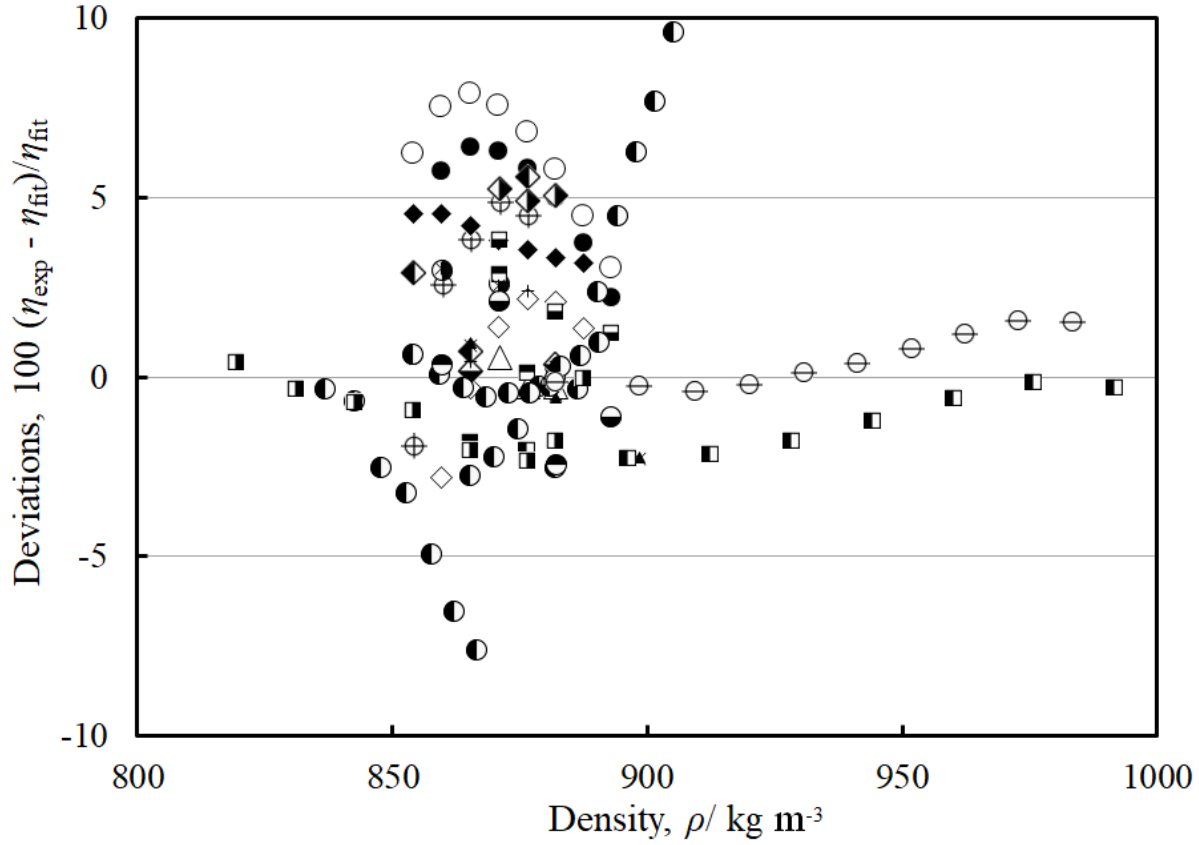

FIG. 6 Relative deviations of the viscosity of primary experimental data of THF from the values calculated by the present scheme, Eqs. 1, 4-8, as a function of density. Al Tuwaim et al. [49] (△), Muhamed et al. [50] (⊕), Droliya and Nain [51] (◇), Chen et al. [52] (◆), Zivkovic et al. [53] (●), Knezevic-Stevanoivic et al. [54] (○), Sinha et al. [55] (◑), Rathnam et al. [56] (⬒), Wankhede et al. [57] (◒), Ku et al. [58] (⬓), Giner et al. [59] (⬙), Nayak et al. [60] (⬖), Nayak et al. [61] (⬗), Postigo et al. [62] (▲), Mariano et al. [63] (x), Muhuri et al. [64] (✶), Zhang and Liu [65] (◐), Oswal [66] (+), Oshmyansky et al. [67] (◓), Metz and Glines [68] (◧), Carvajal et al. [69] (⊖), Kuss [70] (◨).

Table 5 Evaluation of THF viscosity correlation for the secondary data.

Investigators/reference	Year Publ.	AAD (%)	BIAS (%)
Lin et al. [71]	2019	0.23	0.16
Hussain et al. [72]	2019	4.90	4.90
Duereh et al. [73]	2017	2.16	-2.16
Patel et al. [74]	2016	2.15	2.15
Dubey and Kumar [75]	2014	2.68	2.68
Ekka and Roy [76]	2014	0.30	0.30
Elhami-Kalvanagh et al. [77]	2013	3.77	-3.77
Zhu et al. [56]	2011	2.90	2.90
Fattahi and Iloukhani [78]	2010	1.51	-1.49
Bhattacharjee and Roy [79]	2010	0.23	0.23
Rodnikova et al. [80]	2010	37.93	18.17
Al-Kandary et al. [81]	2009	0.13	-0.13
Bandres et al. [82]	2009	0.32	0.32
Mohsen-Nia et al. [83]	2009	1.22	-1.22
Oswal and Ijardar [84]	2009	25.66	-25.66
Palani and Geetha [85]	2009	3.87	3.87
Parveen et al. [86]	2009	1.83	-0.77
Marczak et al. [87]	2008	49.70	49.70
Nain [88]	2007	0.85	-0.85
Zafarani-Moattar and Majdan-Cegincara [89]	2007	2.73	-2.73
Sinha and Roy [90]	2007	0.30	0.30
Sinha and Roy [91]	2007	2.41	2.41
Singh [92]	2006	10.54	10.54
Parmar and Guleria [93]	2006	0.29	-0.29
Tang et al. [94]	2006	0.97	0.97
Gupta et al. [95]	2006	2.29	-1.93
Das and Roy [96]	2006	1.96	1.96
Choudhury et al. [97]	2005	0.71	-0.10
Oswal et al. [98]	2005	0.05	-0.05
Perez et al. [99]	2003	0.56	0.56
Baluga [100]	2002	26.25	26.25
Kinart et al. [101]	2002	1.87	1.87
Saleh et al. [102]	2001	2.53	2.53
Acevedo et al. [103]	2000	0.35	-0.35
Kolosnitsyn et al. [104]	2000	14.02	14.02
Gascon et al. [105]	1999	0.70	0.57
Chauhan et al. [106]	1999	2.90	2.90
Aminabhavi and Patil [107]	1998	2.57	2.57
Aralaguppi et al. [108]	1996	6.76	6.76
Bardavid et al. [109]	1996	1.00	-1.00
Krishnaiah and Surendranath [110]	1996	6.18	6.18
Rodriguez et al. [111]	1996	0.45	0.45
Solimo and Gomez Marigliano [112]	1993	7.18	7.18
Cook et al. [113]	1992	Outside range	
Wencel and Czerepko [114]	1991	23.83	23.83
Ramkumar and Kudchadker [115]	1989	1.64	-1.64
Matsuda et al. [116]	1986	4.90	4.90
Geerissen et al. [117]	1985	1.56	-1.56
Ratkovics and Laszlone Parragi [118]	1984	0.45	-0.45
Gurevich et al. [119]	1982	5.07	5.07
Hayduk et al. [120]	1973	1.70	1.70

Holland and Smyth [121]	1955	4.71	4.71

Finally, Fig. 7 shows a plot of the viscosity of THF as a function of the temperature for different pressures. The plot demonstrates the physically reasonable extrapolation behavior at pressures higher than 30 MPa, and at temperatures that exceed the 353 K limit of the current measurements and the 550 K limit of the Fiedler et al. EOS [2]. Although the correlation does not show unphysical behavior when extrapolated to 100 MPa, the uncertainties above 30 MPa could be very large and we do not recommend using the equation outside of its range of validation (up to 30 MPa) until additional high-pressure data are available for validation of the extrapolation behavior.

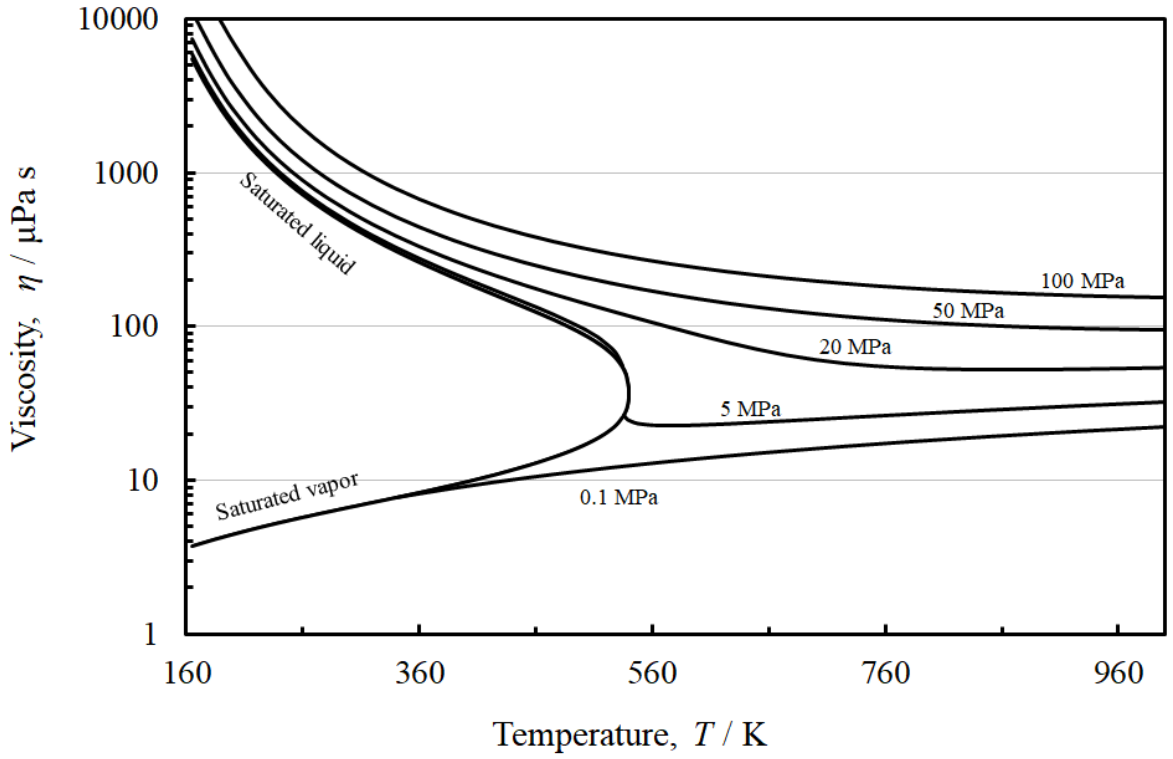

FIG. 7 Viscosity of THF as a function of the temperature for different pressures.

3 The thermal conductivity correlation

In a very similar fashion to that described for the expression of viscosity in Section 2, the thermal conductivity λ is expressed as the sum of three independent contributions, as

$$\lambda(\rho,T) = \lambda_{\mathrm{o}}(T) + \Delta\lambda(\rho,T) + \Delta\lambda_{\mathrm{c}}(\rho,T) \tag{9}$$

where ρ is the density, T is the temperature, and the first term, $\lambda_o(T) = \lambda(0,T)$, is the contribution to the thermal conductivity in the dilute-gas limit, where only two-body molecular interactions occur. The final term, $\Delta\lambda_c(\rho,T)$, the critical enhancement, arises from the long-range density fluctuations that occur in a fluid near its critical point, which contribute to divergence of the thermal conductivity at the critical point. Finally, the term $\Delta\lambda(\rho,T)$, the residual property, represents the contribution of all other effects to the thermal conductivity of the fluid at elevated densities.

Table 6 Thermal conductivity measurements of THF

Investigators/reference	Publ. Year	Technique employed[a]	Purity (%)	Uncer-tainty (%)	No. of data	Temperature range (K)	Pressure range (MPa)
Primary data							
Fan et al. [130]	2022	THW2	99.0	2.0	20	272-332	0.1-15
Lei et al. [131]	1997	THW	99.0	0.7	6	253-303	0.1
Ross and Andersson [132]	1981	THW	na	4.0	26	174-300	110
Secondary data							
Gurevich et al. [133]	1982	na	na	na	5	233-313	0.1

[a] THW, Transient Hot Wire; THW2, Transient Hot-Wire Instrument with 2 wires.
na not available.

Table 6 summarizes, to the best of our knowledge, the experimental measurements of the thermal conductivity of THF reported in the literature. Only 4 sets could be found. The measurements of Gurevich et al. [133] were found to be much higher (factor of 2) then the other measurements and with the opposite temperature slope. Hence, this set was considered as secondary, while remaining measurements formed the primary data set.

Figures 8 and 9 show the ranges of the primary measurements outlined in Table 6, and the phase may be seen as well. The lack of data in the vapor phase, near the critical temperature, and in the supercritical region is apparent. The development of the correlation requires densities. As already discussed in the case of the viscosity correlation, we employed the equation of state of Fiedler et al. [2].

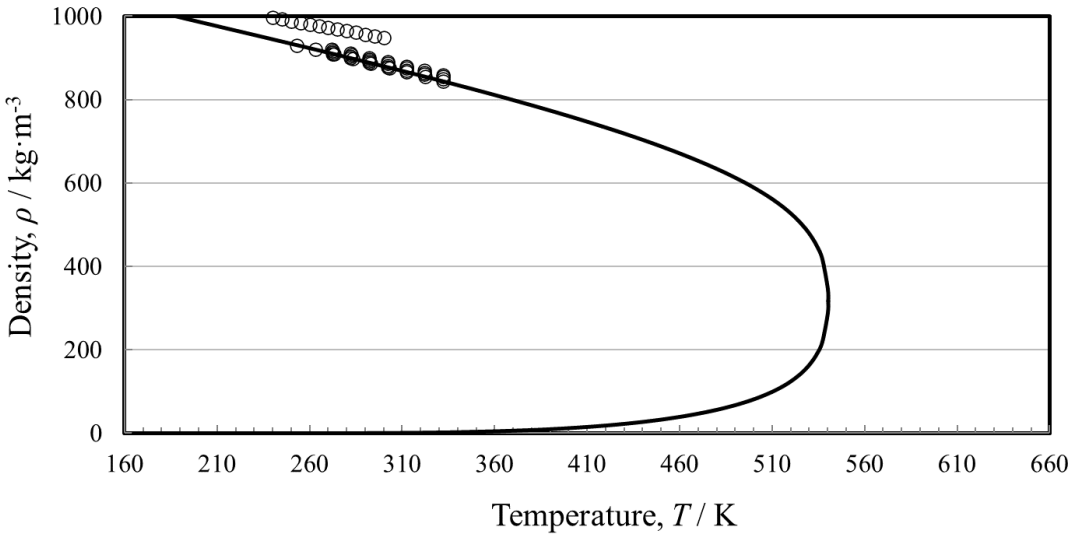

FIG. 8 Temperature-density ranges of the primary experimental thermal conductivity data for THF, (––) saturation curve.

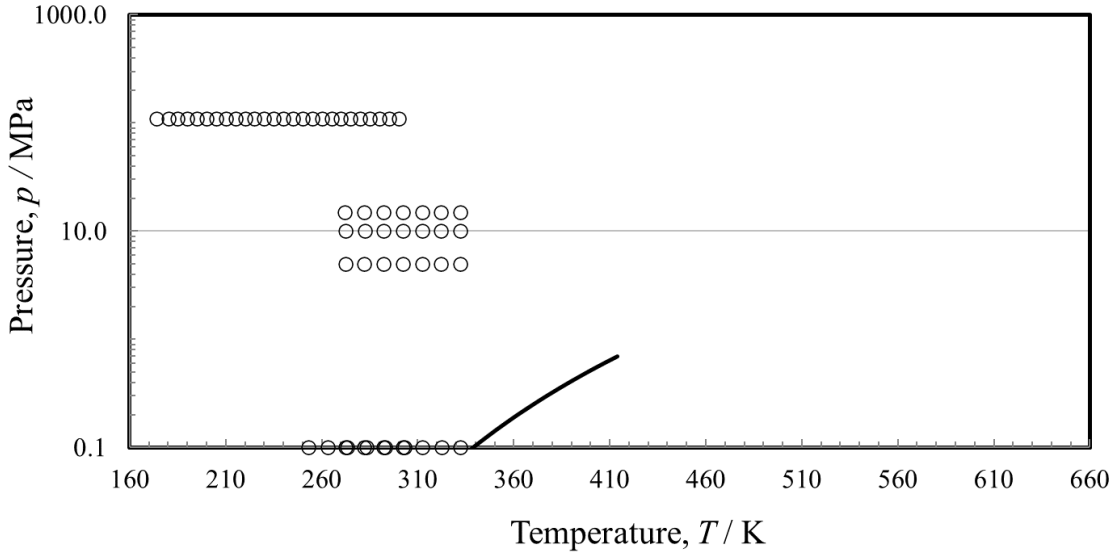

FIG. 9 Temperature-pressure ranges of the primary experimental thermal conductivity data for THF, (—) saturation curve.

3.1 The dilute-gas limit thermal conductivity

The dilute-gas limit thermal conductivity, $\lambda_0(T)$ in $mW \cdot m^{-1} \cdot K^{-1}$, can be analyzed independently of all other contributions in Eq. 9. As there are no measurements in the vapor phase, a theoretically based scheme was used to provide estimated data for the dilute-gas limit thermal conductivity, $\lambda_o(T)$, over a wide temperature range. This same scheme was successfully adopted in the case of the dilute-gas limit thermal conductivity correlation of normal and parahydrogen [25], sulfur hexafluoride [30], toluene [36], benzene [35], *n*-hexane [32] and ethylene glycol [40]. A reasonable estimate of the thermal

conductivity, $\lambda_o(T)$, of a pure dilute gas may be obtained from the viscosity, $\eta_o(T)$, and the ideal-gas heat capacity at constant volume, C_v^0, through the modified Eucken correlation [134]

$$f_{\mathrm{EU}} = \frac{\lambda_0(T)\, M}{\eta_0(T)\, C_v^0} = 1.32 + 1.77\left(\frac{R}{C_v^0}\right). \tag{10}$$

In the above equation, M represents the molar mass of THF (see Table 2), and R the universal gas constant (J·mol·K^{-1}). The ideal-gas isochoric heat capacity C_v^0, can be obtained from the equivalent isobaric heat capacity [2], $C_p^0 = C_v^0 + R$, as

$$\frac{C_p^o}{k_{\mathrm{B}}} = 4 + \sum_{k=1}^{4} v_k \left(\frac{u_k}{T}\right)^2 \frac{\exp(u_k / T)}{\left[\exp(u_k / T) - 1\right]^2}, \tag{11}$$

where k_{B} is the Boltzmann constant (1.380649×10^{-23} J·K^{-1} [135]), and the values of the coefficients v_k and u_k are: v_1 = 18.2, v_2 = 11.394, v_3 = 1.05, v_4 = 2.37, and u_1 = 1460 K, u_2 = 3461 K, u_3 = 11,000 K, u_4 = 517 [2].

The dilute-gas limit thermal conductivity values $\lambda_0(T)$ (mW·m^{-1}·K^{-1}) obtained by Eqs. 10 and 11 were fitted as a function of the reduced temperature, $T_{\mathrm{r}} = T/T_{\mathrm{c}}$, as

$$\lambda_0(T) = \frac{-1.94973 + 19.5154T_{\mathrm{r}} - 63.3241T_{\mathrm{r}}^2 + 87.1979T_{\mathrm{r}}^3 + 12.5447T_{\mathrm{r}}^4 - 7.42725T_{\mathrm{r}}^5 + 0.933011T_{\mathrm{r}}^6}{0.0360636 + 0.13434T_{\mathrm{r}} + T_{\mathrm{r}}^2}. \tag{12}$$

This equation represents the calculated values in the temperature range from the triple point to 1000 K to within 0.1 %. Equation 12 is hence employed in the calculations that will follow. Figure 10 shows the dilute-gas thermal-conductivity values calculated from Eq. 12 as a function of temperature.

However, as the values of the dilute-gas viscosity are from estimation and have a 10 % uncertainty, the thermal conductivity values obtained from Eq. 12 have an estimated uncertainty of about 15 %. This is quite large but is due to the complete lack of gas phase data for both viscosity and thermal conductivity.

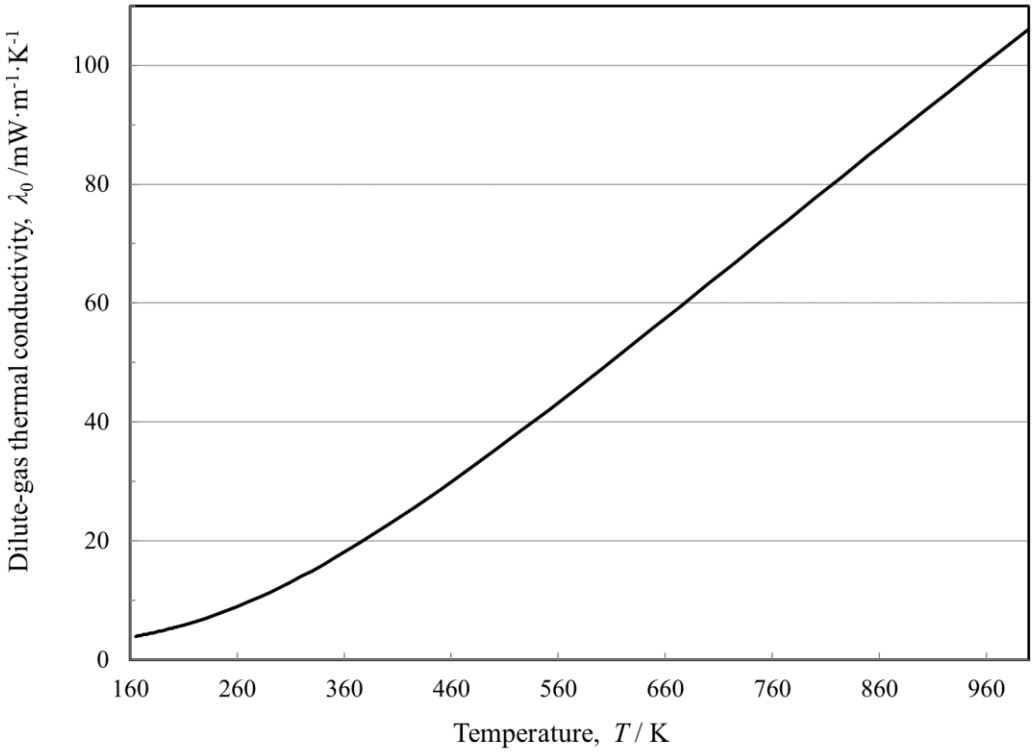

FIG. 10 Dilute-gas thermal conductivity values calculated from Eq. 12, as a function of the temperature

3.2 The thermal conductivity residual term

The thermal conductivities of pure fluids exhibit an enhancement over a large range of densities and temperatures around the critical point and become infinite at the critical point. This behavior can be described by models that produce a smooth crossover from the singular behavior of the thermal conductivity asymptotically close to the critical point to the residual values far away from the critical point [136-138]. The density-dependent terms for thermal conductivity can be grouped according to Eq. 9 as $[\Delta\lambda(\rho,T) + \Delta\lambda_c(\rho,T)]$. To assess the critical enhancement theoretically, we need to evaluate, in addition to the dilute-gas thermal conductivity, the residual thermal-conductivity contribution. The procedure adopted during this analysis used ODRPACK (Ref. [139]) to fit all the primary data simultaneously to the residual thermal conductivity and the critical enhancement, while maintaining the values of the dilute-gas thermal-conductivity data already obtained. The density values employed were obtained by the equation of state of Fiedler et al. [2]. The primary data were weighted in inverse proportion to the square of their uncertainty.

The residual thermal conductivity was represented with a polynomial in temperature and density:

$$\Delta\lambda(\rho,T) = \sum_{i=1}^{5}\left(B_{1,i} + B_{2,i}(T/T_c)\right)\left(\rho/\rho_c\right)^i . \tag{13}$$

Coefficients $B_{1,i}$ and $B_{2,i}$ are shown in Table 7.

Table 7 Coefficients of Eq. 13 for the residual thermal conductivity of THF.

i	$B_{1,i}$ (mW·m^{-1}·K^{-1})	$B_{2,i}$ (mW·m^{-1}·K^{-1})
1	0.137024×10^{-1}	0.767387×10^{-2}
2	0.417645×10^{-1}	-0.491144×10^{-1}
3	-0.442346×10^{-1}	0.579725×10^{-1}
4	0.198436×10^{-1}	-0.284934×10^{-1}
5	-0.278328×10^{-2}	0.495863×10^{-2}

3.3 The thermal conductivity critical enhancement term

The theoretically based crossover model proposed by Olchowy and Sengers [136-138] is complex and requires solution of a quartic system of equations in terms of complex variables. A simplified crossover model has also been proposed by Olchowy and Sengers [140]. The critical enhancement of the thermal conductivity from this simplified model is given by

$$\Delta\lambda_{\rm c} = \frac{\rho c_p R_{\rm D} k_{\rm B} T}{6\pi\bar{\eta}\xi}\left(\bar{\Omega}-\bar{\Omega}_0\right), \tag{14}$$

with

$$\bar{\Omega} = \frac{2}{\pi}\left[\left(\frac{c_p - c_v}{c_p}\right)\arctan\left(\bar{q}_{\rm D}\xi\right) + \frac{c_v}{c_p}\bar{q}_{\rm D}\xi\right] \tag{15}$$

and

$$\bar{\Omega}_0 = \frac{2}{\pi}\left[1-\exp\left(-\frac{1}{(\bar{q}_{\rm D}\xi)^{-1}+(\bar{q}_{\rm D}\xi\rho_{\rm c}/\rho)^2/3}\right)\right]. \tag{16}$$

In Eqs. 14 – 16, $k_{\rm B}$ is the Boltzmann constant, $\bar{\eta}$ (Pa·s) is the viscosity, and c_p and c_v (J·kg^{-1}·K^{-1}) are the isobaric and isochoric specific heat obtained from the equation of state. The correlation length ξ (m) is given by

$$\xi = \xi_0\left(\frac{p_{\rm c}\rho}{\Gamma\rho_{\rm c}^2}\right)^{\nu/\gamma}\left[\left.\frac{\partial\rho(T,\rho)}{\partial p}\right|_T - \left(\frac{T_{\rm ref}}{T}\right)\left.\frac{\partial\rho(T_{\rm ref},\rho)}{\partial p}\right|_T\right]^{\nu/\gamma}. \tag{17}$$

This crossover model requires the universal amplitude, $R_{\rm D}$ = 1.02, and the universal critical exponents, ν = 0.63 and γ =1.239, and the system–dependent amplitudes Γ and ξ_0. For this work, we adopted the values Γ = 0.057 (-), $\xi_0 = 0.207\times10^{-9}$ m, using the universal representation of the critical

enhancement of the thermal conductivity by Perkins *et al*. [141]. We also used this method to estimate the effective cutoff wavelength $\bar{q}_D^{-1}$ (m), and obtained 5.99×10^{-10} m. The viscosity required for Eq. 14 was calculated with the correlation developed earlier in this work. The reference temperature T_{ref}, far above the critical temperature where the critical enhancement is negligible, was calculated by $T_{ref} = (3/2)\, T_c$ [47], which for THF is 810 K. Thus, the present critical enhancement calculation is consistent with the equation of state of Fiedler et al. [2], and should provide reasonable estimates of the thermal conductivity critical enhancement, although the uncertainty is larger in this area.

3.4 Comparison with data

Table 8 summarizes comparisons of the primary data with the correlation. We estimate the uncertainty (at the 95% confidence level) for the thermal conductivity in the liquid phase from the triple-point temperature to 330 K at pressures up to 15 MPa is 2%, rising to 4% at 110 MPa. The agreement with the experimental data is better than that, but the correlation cannot be more accurate than the data upon which it is based. Note that Ross and Andersson [132] claim an uncertainty of 3% for their solid phase measurements but do not explicitly call out an uncertainty for the liquid measurements. They state only that their results for the liquids are less accurate than for solids, and we assigned an uncertainty of 4% to their measurements based on this comment. Uncertainties in the critical region are much larger, since the thermal conductivity approaches infinity at the critical point and is very sensitive to small changes in density. Although the correlation behaves in a physically reasonable manner up to 550 K (the limit of the EOS), the lack of data in this region prevents validation at high temperatures. The reader should also be aware of the possibility of thermal decomposition at high temperatures [142], as this correlation does not take that into account.

Table 8 Evaluation of the THF thermal-conductivity correlation for the primary data.

Investigators/reference	Publ. Year	AAD (%)	BIAS (%)
Fan et al. [130]	2022	0.37	-0.09
Lei et al. [131]	1997	0.97	0.10
Ross and Andersson [132]	1981	0.41	0.20
Total		0.45	0.06

Figure 11 shows the percentage deviations of all primary thermal–conductivity data from the values calculated by Eqs. 9, 12 – 17, as a function of temperature. Figures 12 and 13 show the same deviations but as a function of pressure and density, respectively.

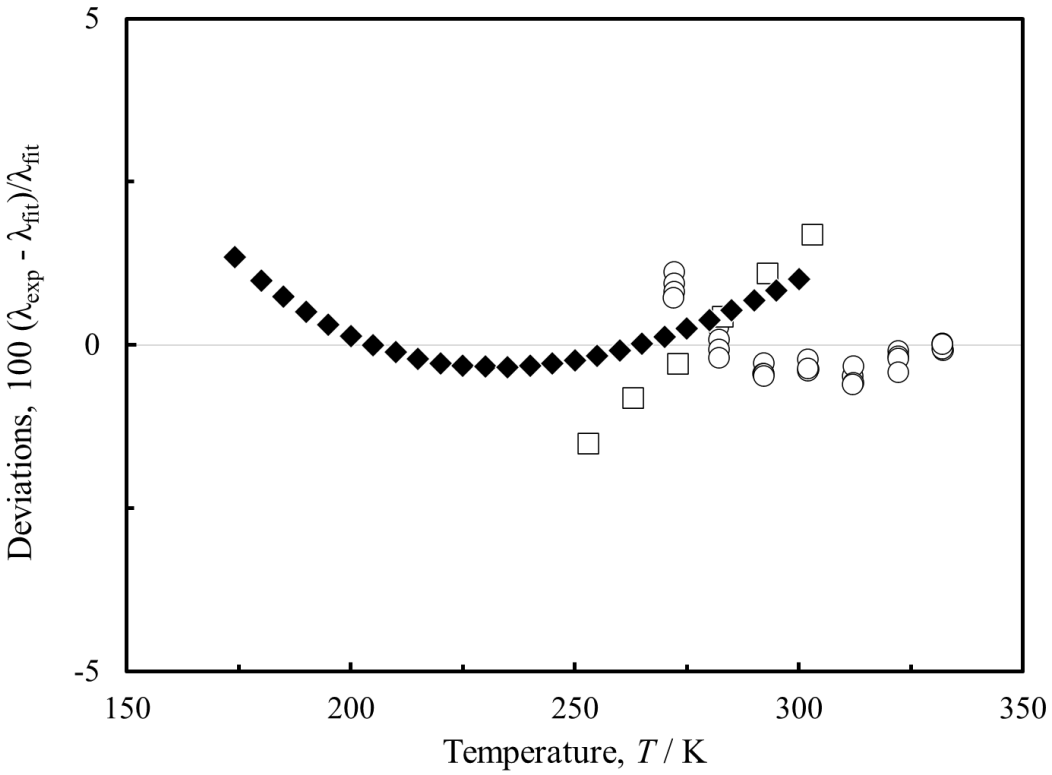

FIG. 11 Percentage deviations of primary thermal conductivity experimental data of THF from the values calculated by the present scheme, Eqs. 9, 12 – 17, as a function of temperature: Fan et al. [130] (○), Lei et al. [131] (□), Ross and Andersson [132] (◆).

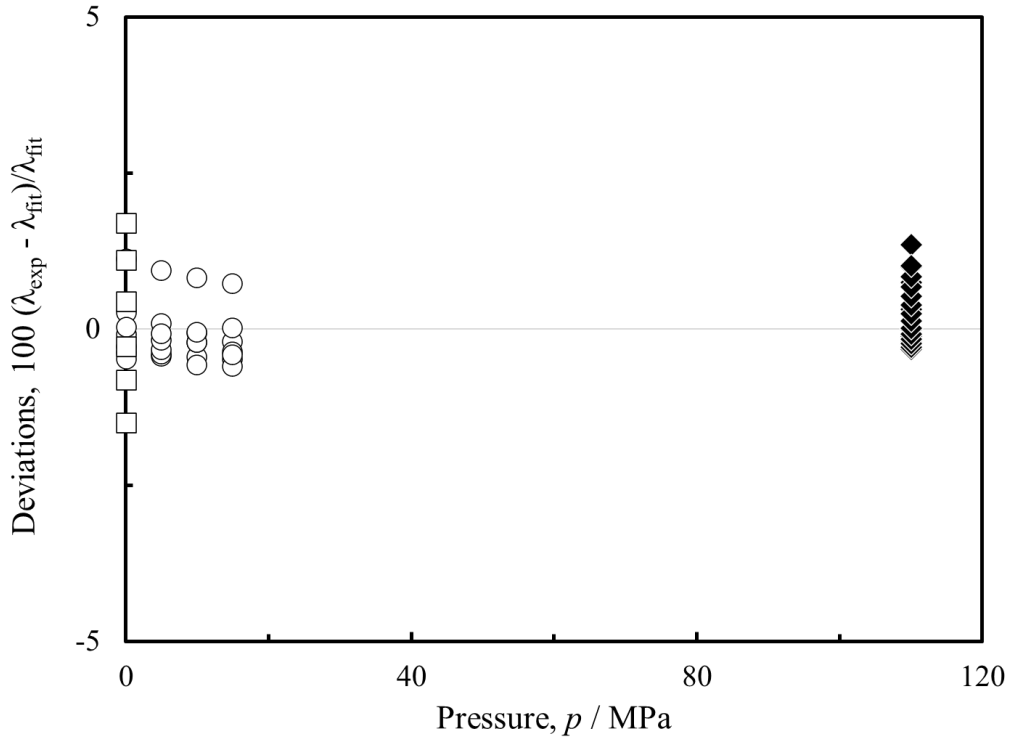

FIG. 12 Percentage deviations of primary thermal conductivity experimental data of THF from the values calculated by the present scheme, Eqs. 9, 12 – 17, as a function of pressure: Fan et al. [130] (○), Lei et al. [131] (□), Ross and Andersson [132] (◆).

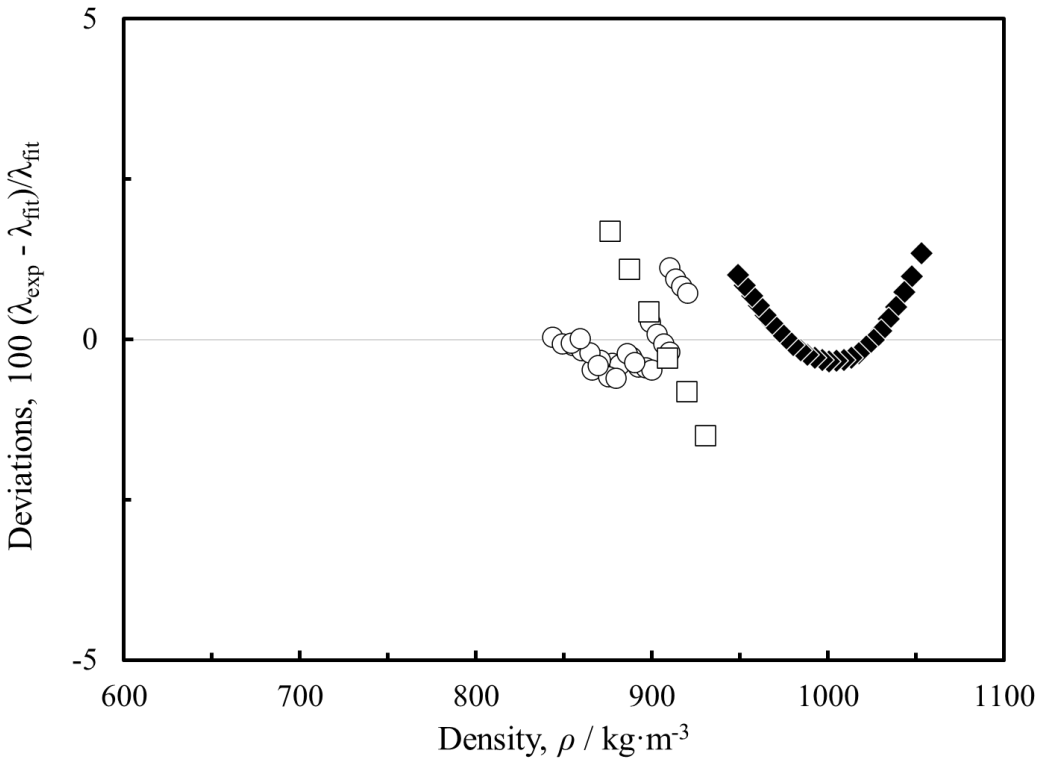

FIG. 13 Percentage deviations of primary thermal conductivity experimental data of THF from the values calculated by the present scheme, Eqs. 9, 12 – 17, as a function of density: Fan et al. [130] (○), Lei et al. [131] (□), Ross and Andersson [132] (◆).

Figure 14 shows a plot of the thermal conductivity of THF as a function of the temperature for different pressures. The plot demonstrates the physically reasonable extrapolation behavior at pressures higher than 110 MPa and at temperatures that exceed the 330 K limit of the current measurements. Finally, Fig. 15 depicts the critical region as calculated by the present correlation.

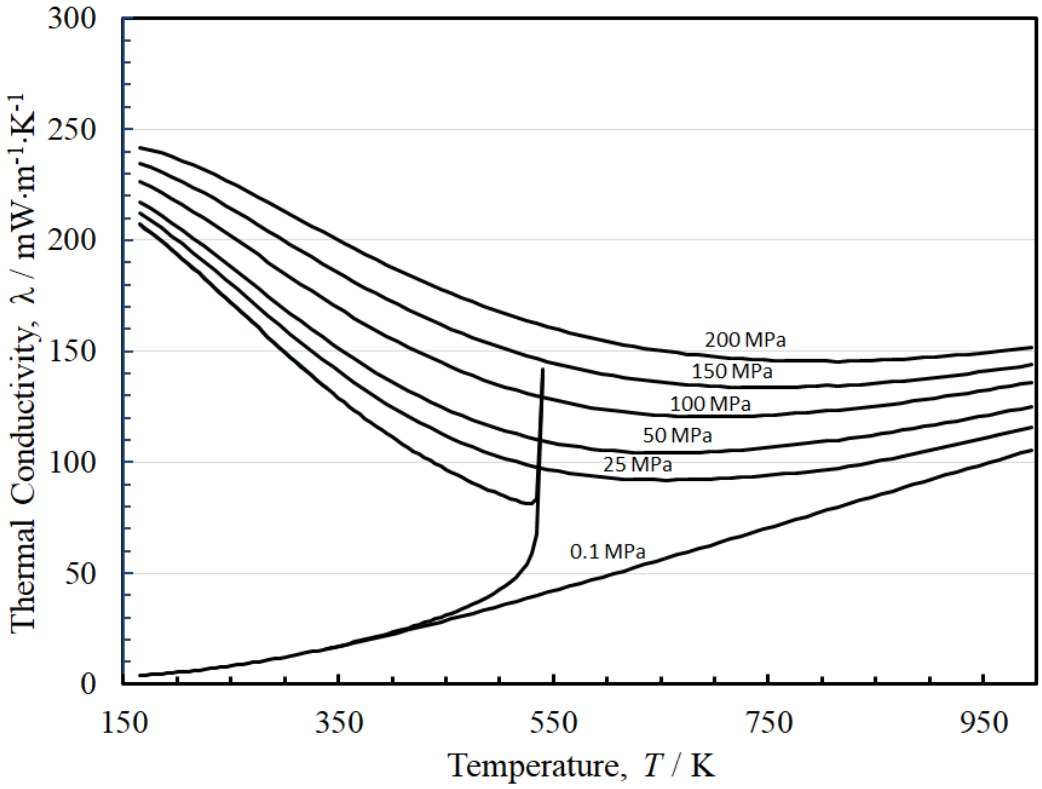

FIG. 14 The thermal conductivity of THF as a function of temperature at different pressures.

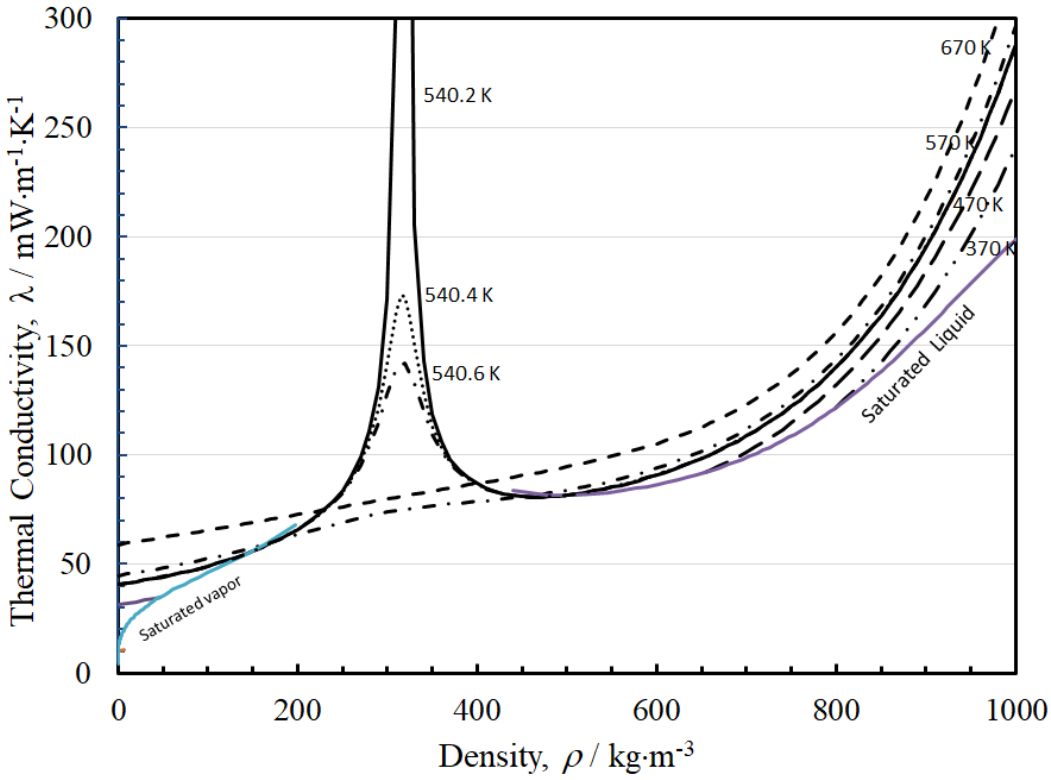

FIG. 15 The thermal conductivity of THF as a function of density at different temperatures

4. Recommended Values and Computer-Program Verification

4.1 Recommended Values

In Table 9, viscosity and thermal conductivity values are given along the saturation boundary, calculated from the present proposed correlation between 200 and 500 K, while in Table 10, viscosity and thermal conductivity values are given for temperatures between 200 and 500 K and at selected pressures. Saturation density values for selected temperatures, as well as the density values for the selected temperature and pressure are obtained from the equation of state of Fiedler et al. [2] as calculated with REFPROP v10 [122] using the supplementary file included with this work. The values in the tables are calculated from the given temperatures and densities according to Eqs.1, 4 – 8 for viscosity and Eqs. 9, 12 – 17 for thermal conductivity.

Table 9 Viscosity and thermal conductivity values of THF along the saturation boundary, calculated by the present scheme.

T (K)	ρ_{liq} ($kg \cdot m^{-3}$)	ρ_{vap} ($kg \cdot m^{-3}$)	η_{liq} ($\mu Pa \cdot s$)	η_{vap} ($\mu Pa \cdot s$)	λ_{liq} ($mW \cdot m^{-1} \cdot K^{-1}$)	λ_{vap} ($mW \cdot m^{-1} \cdot K^{-1}$)
200	986.55	0.00091066	2018.5	5.57	193.7	5.42
250	933.85	0.055411	825.0	6.96	171.9	8.29
300	879.90	0.68415	452.5	8.44	149.7	12.3
350	822.94	3.6651	286.1	10.1	129.0	17.3
400	760.49	12.424	195.1	12.1	111.2	23.4
450	687.67	32.984	137.4	14.9	96.8	31.1
500	589.08	81.621	93.8	19.7	85.6	42.5

Table 10 Viscosity and thermal conductivity values of THF at selected temperatures and pressures, calculated by the present scheme.

p (MPa)	T (K)	ρ (kg·m^{-3})	η (μPa·s)	λ (mW·m^{-1}·K^{-1})
0.1	200	986.60	2021.1	193.8
	250	933.91	826.0	172.0
	300	879.97	452.9	149.7
	350	2.5418	10.04	17.2
	400	2.2048	11.56	22.7
	450	1.9497	13.04	28.8
	500	1.7489	14.49	35.3
10	200	991.26	2290.9	196.4
	250	940.08	920.6	175.4
	300	888.43	504.8	153.9
	350	834.98	322.3	134.1
	400	778.12	224.1	117.0
	450	715.04	163.1	103.2
	500	639.54	119.8	92.6
25	200	997.97	2768.9	200.2
	250	948.79	1080.1	180.2
	300	899.99	589.3	159.9
	350	850.70	379.5	141.0
	400	800.14	269.1	124.9
	450	747.42	203.0	112.0
	500	691.46	159.4	102.5
50	200	1008.4		206.3
	250	961.93		187.9
	300	916.78		169.0
	350	872.33		151.4
	400	828.21		136.2
	450	784.15		124.0
	500	740.06		114.9
100	200	1026.9		217.4
	250	984.50		201.8
	300	944.29		185.2
	350	905.78		169.5
	400	868.66		155.5
	450	832.77		143.9
	500	798.04		134.7

4.2 Computer-Program Verification

For checking computer implementations of the correlation, the following points may be used for the given T, ρ conditions: T = 300 K, ρ = 0 kg·m^{-3}, η = 8.3705 μPa·s, and λ = 12.2206 mW·m^{-1}·K^{-1}, while for T = 300 K, ρ = 900.0 kg m^{-3}, η = 589.3956 μPa·s, and λ = 159.8654 mW·m^{-1}·K^{-1}. (for this point there is a very small contribution of 0.0408 mW·m^{-1}·K^{-1} to λ from the critical enhancement term).

5 Conclusions

A new hybrid prediction-correlation scheme for the viscosity and thermal conductivity of THF is presented. The scheme for the liquid phase is based on critically evaluated experimental data, but the gas phase as well as the supercritical phase are entirely predictive since there were no data in these regions. Both correlations are designed to be used with a recently published equation of state [2] that extends from the triple-point temperature to 550 K, at pressures up to 600 MPa.

The viscosity correlation is validated from 195 K to 353 K, and up to 30 MPa pressure, while the thermal conductivity is validated in the temperature range 174 K to 332 K, and up to 110 MPa pressure. The estimated uncertainty (at a 95% confidence level) for the viscosity is 10% for the low-density gas (up to atmospheric pressure), and 6% for the liquid at temperatures up to 353 K and pressures up to 30 MPa. For thermal conductivity, the expanded uncertainty is estimated to be 15% for the low-density gas and 2% for the liquid at pressures up to 15 MPa, rising to 4% at 110 MPa. Due to the extremely limited data available, both correlations should be considered preliminary until further experimental data become available.

Declarations

Author Contributions

All authors contributed equally in preparing and reviewing this manuscript.

Funding

This study was partially supported by the National Institute of Standards and Technology.

Conflict of interest

One of the authors (Marc J. Assael) declares that he is the Editor-in-Chief of the International Journal of Thermophysics.

Supplementary information

Supplementary Information The online version contains supplementary material available at https:// …….

Supplementary file THF.txt text file containing the parameters for the calculation of the thermophysical properties of THF including the viscosity and the thermal conductivity correlations in this work is available for use with the REFPROP [122] computer program. It must be named with the extension .FLD (for example THF.FLD) to be viewed properly by the REFPROP program (TXT 40 kb).

6 References

1. V.J. Ram, A. Sethi, M. Nath, R. Pratap, Chapter 5. Five-Membered Heterocycles in The Chemistry of Heterocycles. Nomenclature and Chemistry of Three-to-Five Membered Heterocycles (Elsevier, 2019)
2. F. Fiedler, J. Karog, E.W. Lemmon, M. Thol, Int. J. Thermophys. 44, 153 (2023) - Erratum: Int. J. Thermophys. 44, 175 (2023). https://doi.org/10.1007/s10765-023-03258-3
3. D. Velliadou, K. Tasidou, K.D. Antoniadis, M.J. Assael, R.A. Perkins, M.L. Huber, Int. J. Thermophys. 42, 74 (2021). https://doi.org/10.1007/s10765-021-02818-9
4. M.L. Huber, R.A. Perkins, A. Laesecke, D.G. Friend, J.V. Sengers, M.J. Assael, I.N. Metaxa, E. Vogel, R. Mares, K. Miyagawa, J. Phys. Chem. Ref. Data 38, 101 (2009). https://doi.org/10.1063/1.3088050
5. S.A. Monogenidou, M.J. Assael, M.L. Huber, J. Phys. Chem. Ref. Data 47, 023102 (2018). https://doi.org/10.1063/1.5036724
6. M.J. Assael, S.A. Monogenidou, M.L. Huber, R.A. Perkins, J.V. Sengers, J. Phys. Chem. Ref. Data 50, 033102 (2021). https://doi.org/10.1063/5.0048711
7. E.K. Michailidou, M.J. Assael, M.L. Huber, R.A. Perkins, J. Phys. Chem. Ref. Data 42, 033104 (2013). https://doi.org/10.1063/1.4818980
8. E.K. Michailidou, M.J. Assael, M. Huber, I. Abdulagatov, R.A. Perkins, J. Phys. Chem. Ref. Data 43, 023103 (2014). https://doi.org/10.1063/1.4875930
9. M.J. Assael, T.B. Papalas, M.L. Huber, J. Phys. Chem. Ref. Data 46, 033103 (2017). https://doi.org/10.1063/1.4996885
10. S.A. Monogenidou, M.J. Assael, M.L. Huber, J. Phys. Chem. Ref. Data 47, 013103 (2018). https://doi.org/10.1063/1.5021459
11. S. Avgeri, M.J. Assael, M.L. Huber, R.A. Perkins, J. Phys. Chem. Ref. Data 43, 033103 (2014). https://doi.org/10.1063/1.4892935
12. S. Avgeri, M.J. Assael, M.L. Huber, R.A. Perkins, J. Phys. Chem. Ref. Data 44, 033101 (2015). https://doi.org/10.1063/1.4926955
13. K. Tasidou, M.L. Huber, M.J. Assael, J. Phys. Chem. Ref. Data 48, 043101 (2019). https://doi.org/10.1063/1.5128321
14. S. Sotiriadou, E. Ntonti, D. Velliadou, M.J. Assael, M.L. Huber, Int. J. Thermophys. 44, 108 (2023). https://doi.org/10.1007/s10765-023-03217-y
15. E.A. Sykioti, M.J. Assael, M.L. Huber, R.A. Perkins, J. Phys. Chem. Ref. Data 42, 043101 (2013). https://doi.org/10.1063/1.4829449
16. S. Sotiriadou, E. Ntonti, D. Velliadou, K.D. Antoniadis, M.J. Assael, M.L. Huber, Int. J. Thermophys. 40, 44 (2023) - Erratum: Int. J. Thermophys. 44, 46 (2023). https://doi.org/10.1007/s10765-022-03149-z

17. M. Mebellis, D. Velliadou, M.J. Assael, M.L. Huber, Int. J. Thermophys. 42, 116 (2021). https://doi.org/10.1007/s10765-021-02867-0
18. D. Velliadou, K.D. Antoniadis, M.J. Assael, M.L. Huber, Int. J. Thermophys. 43, 42 (2022). https://doi.org/10.1007/s10765-021-02970-2
19. M.L. Huber, M.J. Assael, Int. J. Refrig. 71, 39 (2016). https://doi.org/10.1016/j.ijrefrig.2016.08.007
20. D. Velliadou, M.J. Assael, M.L. Huber, Int. J. Thermophys. 43, 105 (2022). https://doi.org/10.1007/s10765-022-03029-6
21. C.M. Tsolakidou, M.J. Assael, M.L. Huber, R.A. Perkins, J. Phys. Chem. Ref. Data 46, 023103 (2017). https://doi.org/10.1063/1.4983027
22. R.A. Perkins, M.L. Huber, M.J. Assael, J. Chem. Eng. Data 61, 3286 (2016). https://doi.org/10.1021/acs.jced.6b00350
23. D. Velliadou, K.D. Antoniadis, M.J. Assael, M.L. Huber, Int. J. Thermophys. 43, 129 (2022). https://doi.org/10.1007/s10765-022-03050-9
24. D. Velliadou, K.D. Antoniadis, M.J. Assael, M.L. Huber, Int. J. Thermophys. 42, 51 (2021). https://doi.org/10.1007/s10765-021-02803-2
25. M.J. Assael, J.A.M. Assael, M.L. Huber, R.A. Perkins, Y. Takata, J. Phys. Chem. Ref. Data 40, 033101 (2011). https://doi.org/10.1063/1.3606499
26. M.L. Huber, R.A. Perkins, D.G. Friend, J.V. Sengers, M.J. Assael, I.N. Metaxa, K. Miyagawa, R. Hellmann, E. Vogel, J. Phys. Chem. Ref. Data 41, 033102 (2012). https://doi.org/10.1063/1.4738955
27. M.L. Huber, R.A. Perkins, M.J. Assael, S.A. Monogenidou, R. Hellmann, J.V. Sengers, J. Phys. Chem. Ref. Data 51, 013102 (2022). https://doi.org/10.1063/5.0084222
28. M.L. Huber, E.A. Sykioti, M.J. Assael, R.A. Perkins, J. Phys. Chem. Ref. Data 45, 013102 (2016). https://doi.org/10.1063/1.4940892
29. S.A. Monogenidou, M.J. Assael, M.L. Huber, J. Phys. Chem. Ref. Data 47, 043101 (2018). https://doi.org/10.1063/1.5053087
30. M.J. Assael, I.A. Koini, K.D. Antoniadis, M.L. Huber, I.M. Abdulagatov, R.A. Perkins, J. Phys. Chem. Ref. Data 41, 023104 (2012) - Erratum: J. Phys. Chem. Ref. Data 43, 039901 (2014). https://doi.org/10.1063/1.4708620
31. C.-M. Vassiliou, M.J. Assael, M.L. Huber, R.A. Perkins, J. Phys. Chem. Ref. Data 44, 033102 (2015). https://doi.org/10.1063/1.4927095
32. M.J. Assael, S.K. Mylona, C.A. Tsiglifsi, M.L. Huber, R.A. Perkins, J. Phys. Chem. Ref. Data 42, 013106 (2013). https://doi.org/10.1063/1.4793335
33. M.J. Assael, I. Bogdanou, S.K. Mylona, M.L. Huber, R.A. Perkins, V. Vesovic, J. Phys. Chem. Ref. Data 42, 023101 (2013). https://doi.org/10.1063/1.4794091
34. M.J. Assael, A. Koutian, M.L. Huber, R.A. Perkins, J. Phys. Chem. Ref. Data 45, 033104 (2016). https://doi.org/10.1063/1.4958984

35. M.J. Assael, E.K. Michailidou, M.L. Huber, R.A. Perkins, J. Phys. Chem. Ref. Data 41, 043102 (2012). https://doi.org/10.1063/1.4755781
36. M.J. Assael, S.K. Mylona, M.L. Huber, R.A. Perkins, J. Phys. Chem. Ref. Data 41, 023101 (2012). https://doi.org/10.1063/1.3700155
37. S.K. Mylona, K.D. Antoniadis, M.J. Assael, M.L. Huber, R.A. Perkins, J. Phys. Chem. Ref. Data 43, 043104 (2014). https://doi.org/10.1063/1.4901166
38. A. Koutian, M.J. Assael, M.L. Huber, R.A. Perkins, J. Phys. Chem. Ref. Data 46, 013102 (2016). https://doi.org/10.1063/1.4974325
39. M.J. Assael, E.A. Sykioti, M.L. Huber, R.A. Perkins, J. Phys. Chem. Ref. Data 42, 023102 (2013). https://doi.org/10.1063/1.4797368
40. M. Mebellis, D. Velliadou, M.J. Assael, K.D. Antoniadis, M.L. Huber, Int. J. Thermophys. 42, 151 (2021). https://doi.org/10.1007/s10765-021-02904-y
41. R.A. Perkins, M.L. Huber, M.J. Assael, J. Chem. Eng. Data 62, 2659 (2017). https://doi.org/10.1021/acs.jced.7b00106
42. R.A. Perkins, M.L. Huber, M.J. Assael, Int. J. Thermophys. 43, 12 (2021). https://doi.org/10.1007/s10765-021-02941-7
43. M.J. Assael, A.E. Kalyva, S.A. Monogenidou, M.L. Huber, R.A. Perkins, D.G. Friend, E.F. May, J. Phys. Chem. Ref. Data 47, 021501 (2018). https://doi.org/10.1063/1.5036625
44. D.G. Friend, J.C. Rainwater, Chem. Phys. Lett. 107, 590 (1984). https://doi.org/10.1016/S0009-2614(84)85163-5
45. J.C. Rainwater, D.G. Friend, Phys. Rev. A 36, 4062 (1987). https://doi.org/10.1103/physreva.36.4062
46. E. Bich, E. Vogel, Chap. 5.2, in Transport Properties of Fluids. Their Correlation, Prediction and Estimation (Cambridge University Press, Cambridge, 1996)
47. V. Vesovic, W.A. Wakeham, G.A. Olchowy, J.V. Sengers, J.T.R. Watson, J. Millat, J. Phys. Chem. Ref. Data 19, 763 (1990). https://doi.org/10.1063/1.555875
48. S. Hendl, J. Millat, E. Vogel, V. Vesovic, W.A. Wakeham, J. Luettmer-Strathmann, J.V. Sengers, M.J. Assael, Int. J. Thermophys. 15, 1 (1994). https://doi.org/10.1007/BF01439245
49. M.S. AI Tuwaim, A.S. Al-Jimaz, K.H.A.E. Alkhaldi, J. Sol. Chem. 47, 449 (2018). https://doi.org/10.1007/s10953-018-0731-2
50. R.R. Muhamed, R. Rajesh, V. Kannappan, S. Arulappan, A. Prabaharan, J. Mol. Liq. 244, 405 (2017). https://doi.org/10.1016/j.molliq.2017.08.068
51. P. Droliya, A.K. Nain, J. Mol. Liq. 241, 549 (2017). https://doi.org/10.1016/j.molliq.2017.06.021
52. F. Chen, Z. Yang, Z. Chen, J. Hu, C. Chen, J. Cai, J. Mol. Liq. 209, 683 (2015). https://doi.org/10.1016/j.molliq.2015.06.041
53. E.M. Zivkovic, D.M. Bajic, I.R. Radovic, S.P. Serbanovic, M.L. Kijevcanin, Fluid Phase Equilib. 373, 1 (2014). https://doi.org/10.1016/j.fluid.2014.04.002

54. A.B. Knezevic-Stevanoivic, J.D. Smiljanic, S.P. Serbanovic, I.R. Radovic, M.L. Kijevcanin, J. Serb. Chem. Soc 79, 77 (2014). https://doi.org/10.2298/JSC130407045K
55. B. Sinha, R. Pradhan, S. Saha, D. Brahman, A. Sarkar, J. Serb. Chem. Soc 78, 1443 (2013). https://doi.org/10.2298/JSC121210031S
56. M.V. Rathnam, D.R. Ambavadekar, M. Nandini, J. Mol. Liq. 187, 58 (2013). https://doi.org/10.1016/j.molliq.2013.06.002
57. D.S. Wankhede, N.N. Wankhede, B.R. Arbad, M.K. Lande, Int. J. Thermophys. 31, 2239 (2010). https://doi.org/10.1007/s10765-010-0860-3
58. H.-C. Ku, C.-C. Wang, C.-H. Tu, J. Chem. Eng. Data 53, 566 (2008). https://doi.org/10.1021/je700626v
59. B. Giner, I. Gascon, A. Villares, P. Cea, C. Lafuente, J. Chem. Eng. Data 51, 1321 (2006). https://doi.org/10.1021/je0600653
60. J.N. Nayak, M.I. Aralaguppi, B.V.K. Naidu, T.M. Aminabhavi, J. Chem. Eng. Data 49, 468 (2004). https://doi.org/10.1021/je030196t
61. J.N. Nayak, M.I. Aralaguppi, U.S. Toti, T.M. Aminabhavi, J. Chem. Eng. Data 48, 1483 (2003). https://doi.org/10.1021/je030147g
62. M. Postigo, A. Mariano, L. Mussari, A. Camacho, J. Urieta, Fluid Phase Equilib. 207, 193 (2003). https://doi.org/10.1016/S0378-3812(03)00021-9
63. A. Mariano, A. Camacho, M. Postigo, A. Valen, H. Artigas, F.M. Royo, J.S. Urieta, Braz. J. Chem. Eng. 17, 459 (2000). https://dx.doi.org/10.1590/S0104-66322000000400011
64. P.K. Muhuri, B. Das, D.K. Hazra, J. Chem. Eng. Data 41, 1473 (1996). https://doi.org/10.1021/je960196b
65. J. Zhang, H. Liu, J. Chem. Ind. Engin. (Chinese) 42, 269 (1991).
66. S.L. Oswal, Ind. J. Technol. 26, 389 (1988).
67. Y. Oshmyansky, H.J.M. Hanley, J.F. Ely, A.J. Kidnay, Int. J. Thermophys. 7, 599 (1986). https://doi.org/10.1007/BF00502393
68. D.J. Metz, A. Glines, J. Phys. Chem. 71, 1158 (1967). https://doi.org/10.1021/j100863a067
69. C. Carvajal, K.J. Tolle, J. Smid, M. Szwarc, J. Am. Chem. Soc. 87, 5548 (1965). https://doi.org/10.1021/ja00952a005
70. E. Kuss, Z. Angew. Phys. 7, 372 (1955).
71. M.-J. Lin, C.-S. Su, T.-M. Yang, J.-S. Li, J. Chin. Inst. Eng., 42, 420 (2019). https://doi.org/10.1080/02533839.2019.1598285
72. S.G.M. Hussain, R. Kumar, M.M.N. Ali, V. Kannappan, J. Mol. Liq. 277, 865 (2019). https://doi.org/10.1016/j.molliq.2019.01.015
73. A. Duereh, Y. Sato, R.L. Smith Jr., H. Inomata, F. Pichierri, J. Phys. Chem. B 121, 6033 (2017). https://doi.org/10.1021/acs.jpcb.7b03446
74. C.B. Patel, D. Bhavin, P.H. Parsania, J. Indian Chem. Soc. 92 (1395-1407), 1395 (2015).

75. G.P. Dubey, R. Kumar, J. Chem. Thermodyn. 71, 27 (2014). https://doi.org/10.1016/j.jct.2013.10.025
76. D. Ekka, M.N. Roy, Ionics 20, 495 (2014). https://doi.org/10.1007/s11581-013-1003-1
77. R. Elhami-Kalvanagh, H. Shekaari, A. Kazempour, Fluid Phase Equilib. 352, 22 (2013). http://dx.doi.org/10.1016/j.fluid.2013.05.001
78. M. Fattahi, H. Iloukhani, J. Chem. Thermodyn. 42, 1335 (2010). https://doi.org/10.1016/j.jct.2010.05.009
79. A. Bhattacharjee, M.N. Roy, Phys. Chem. Liq. 48, 618 (2010). https://doi.org/10.1080/00319100903350167
80. M.N. Rodnikova, V.M. Troitskii, D.B. Kayumova, I.A. Solonina, M.A. Gunina, Russ. J. Phys. Chem. A 84, 2190 (2010). https://doi.org/10.1134/S0036024410120320
81. J.A. Al-Kandary, A.S. Al-Jimaz, A.M. Abdul-Latif, Phys. Chem. Liq. 47, 210 (2009). https://doi.org/10.1080/00319100802123152
82. I. Bandres, I. Giner, M.E. Aldea, P. Cea, C. Lafuente, Thermochim. Acta 484, 22 (2009). https://doi.org/10.1016/j.tca.2008.11.009
83. M. Mohsen-Nia, H. Modarress, F. Alimohammady, J. Chem. Eng. Data 54, 1375 (2009). https://doi.org/10.1021/je800479m
84. S.L. Oswal, S.P. Ijardar, Thermochim. Acta 496, 97 (2009). https://doi.org/10.1016/j.tca.2009.02.005
85. R. Palani, A. Geetha, Phys. Chem. Liq. 47, 542 (2009). https://doi.org/10.1080/00319100802562862
86. S. Parveen, D. Shukla, S. Singh, K.P. Singh, M. Gupta, J.P. Shukla, Appl. Acoust. 70, 507 (2009). https://doi.org/10.1016/j.apacoust.2008.05.008
87. W. Marczak, M. Sajewicz, M. Bucek, D. Piotrowski, K. Szewczyk, T. Kowalska, J. Mol. Liq. 141, 8 (2008). https://doi.org/10.1016/j.molliq.2008.02.004
88. A.K. Nain, Phys. Chem. Liq. 45, 371 (2007). http://doi.org/10.1080/00319100701230405
89. M.T. Zafarani-Moattar, R. Majdan-Cegincara, J. Chem. Eng. Data 52, 2359 (2007). https://doi.org/10.1021/je700338t
90. A. Sinha, M.N. Roy, Phys. Chem. Liq. 45, 67 (2007). https://doi.org/10.1080/00319100601153830
91. A. Sinha, M.N. Roy, J. Chem. Eng. Data 51, 1415 (2006). https://doi.org/10.1021/je060113j
92. M. Singh, J. Biochem. Biophys. Methods 67, 151 (2006). https://doi.org/10.1016/j.jbbm.2006.02.008
93. M.L. Parmar, M.K. Guleria, J. Mol. Liq. 126, 48 (2006). https://doi.org/10.1016/j.molliq.2005.07.002
94. S.-Y. Tang, D.-Z. Liu, J.-J. Wang, H.-Y. Wang, J. Chem. Eng. Data 51, 2255 (2006). https://doi.org/10.1021/je0603372

95. M. Gupta, I. Vibhu, J.P. Shukla, Fluid Phase Equilib. 244, 26 (2006). https://doi.org/10.1016/j.fluid.2005.07.013
96. M. Das, M.N. Roy, J. Chem. Eng. Data 51, 2225 (2006). https://doi.org/10.1021/je060311a
97. A. Choudhury, M. Das, M.N. Roy, J. Indian Chem. Soc. 82, 625 (2005).
98. S.L. Oswal, R.L. Gardas, R.P. Phalak, Thermochim. Acta 426, 199 (2005). https://doi.org/10.1016/j.tca.2004.08.001
99. E. Perez, M. Cardoso, A.M. Mainar, J.I. Pardo, J.S. Urieta, J. Chem. Eng. Data 48, 1306 (2003). https://doi.org/10.1021/je034076x
100. S. Baluja, J. Indian Chem. Soc. 79, 142 (2002).
101. C.M. Kinart, W.J. Kinart, A. Cwiklinska, J. Therm. Anal. Calorim. 68, 307 (2002). https://doi.org/10.1023/A:1014981921097
102. M.A. Saleh, S. Akhtar, M. Shamsuddin, M.H. Uddin, Phys. Chem. Liq. 39, 551 (2001). https://doi.org/10.1080/00319100108030677
103. I.L. Acevedo, G.C. Pedrosa, M. Katz, L. Mussari, M.A. Postigo, J. Sol. Chem. 29, 1237 (2000). https://doi.org/10.1023/A:1026488212988
104. V.S. Kolosnitsyn, N.V. Slobodchikova, L.V. Sheina, Zh.Prikl. Khim. 73, 1089 (2000).
105. I. Gascon, C. Lafuente, P. Cea, F.M. Royo, J.S. Urieta, Fluid Phase Equilib. 164, 143 (1999). https://doi.org/10.1016/S0378-3812(99)00257-5
106. M.S. Chauhan, A. Kumar, S. Chauhan, Acoustics Lett. 21, 228 (1999).
107. T.M. Aminabhavi, V.B. Patil, J. Chem. Eng. Data 43, 497 (1998). https://doi.org/10.1021/je980031y
108. M.I. Aralaguppi, C.V. Jadar, T.M. Aminabhavi, J. Chem. Eng. Data 41, 1307 (1996). https://doi.org/10.1021/je960133t
109. S.M. Bardavid, G.C. Pedrosa, M. Katz, M.A. Postigo, P. Garcia, J. Sol. Chem. 25, 1125 (1996). https://doi.org/10.1007/BF00972927
110. A. Krishnaiah, K.N. Surendranath, J. Chem. Eng. Data 41, 1012 (1996). https://doi.org/10.1021/je950304e
111. S. Rodriguez, C. Lafuente, J.A. Carrion, F.M. Royo, J.S. Urieta, Int. J. Thermophys. 17, 1281 (1996). https://doi.org/10.1007/BF01438670
112. H.N. Solimo, A.C. Gomez Marigliano, J. Sol. Chem. 22, 951 (1993). https://doi.org/10.1007/BF00646606
113. R.L. Cook, H.E.J. King, D.G. Peiffer, Macromolecules 25, 2928 (1992). https://doi.org/10.1021/ma00037a022
114. A. Wencel, K. Czerepko, Pol. J. Chem. 65, 1809 (1991).
115. D.H.S. Ramkumar, A.P. Kudchadker, J. Chem. Eng. Data 34, 463 (1989). https://doi.org/10.1021/je00058a027
116. Y. Matsuda, M. Morita, R. Tachihara, Bull. Chem. Soc. Japan 59, 1967 (1986). https://doi.org/10.1246/bcsj.59.1967

117. H. Geerissen, J. Roos, B.A. Wolf, Makromol. Chem. 186, 787 (1985).
118. F. Ratkovics, M. Laszlone Parragi, Magy. Kem. Foly. 90, 28 (1984).
119. I.G. Gurevich, K.B. Gisina, V.K. Shitnikov, V.S. Dubasova, V.L. Nikonov, Inzh. Fiz. Zh. 42, 422 (1982).
120. W. Hayduk, H. Laudie, O.H. Smith, J. Chem. Eng. Data 18, 373 (1973). https://doi.org/10.1021/je60059a027
121. R.S. Holland, C.P. Smyth, J. Phys. Chem. 59, 1088 (1955). https://doi.org/10.1021/j150532a025
122. E.W. Lemmon, I.H. Bell, M.L. Huber, M.O. McLinden, (REFPROP, NIST Standard Reference Database 23,Version 10.0, NIST, Standard Reference Data Program, Gaithersburg, MD (2018) https://doi.org/10.18434/T4/1502528),
123. E. Vogel, C. Küchenmeister, E. Bich, A. Laesecke, J. Phys. Chem. Ref. Data 27, 947 (1998). https://doi.org/10.1063/1.556025
124. P.D. Neufeld, A.R. Janzen, R.A. Aziz, J. Chem. Phys. 57, 1100 (1972). https://doi.org/10.1063/1.1678363
125. T.-H. Chung, M. Ajlan, L.L. Lee, K.E. Starling, Ind. Eng. Chem. Res. 27, 671 (1988). https://doi.org/10.1021/ie00076a024
126. FindGraph, v2.611, UNIPHIZ Lab, 2002 - 2015, Certain equipment, instruments, software, or materials are identified in this paper in order to specify the experimental procedure adequately. Such identification is not intended to imply recommendation or endorsement of any product or service by NIST, nor is it intended to imply that the materials or equipment identified are necessarily the best available for the purpose.
127. E. Vogel, E. Bich, R. Nimz, Phys. A 139, 188 (1986). https://doi.org/10.1016/0378-4371(86)90012-9
128. EUREQA Formulize v.098.1, Nutonian Inc., Cambridge MA, USA (Nutonian Inc., Cambridge MA, USA)
129. M.J. Assael, J.H. Dymond, M. Papadaki, P.M. Patterson, Int. J. Thermophys. 13, 269 (1992). https://doi.org/10.1007/BF00504436
130. J. Fan, P. Liu, Z. Gao, F. Song, Fluid Phase Equilib. 551, 113288 (2022). https://doi.org/10.1016/j.fluid.2021.113288
131. Q.-F. Lei, R.-S. Lin, D.-Y. Ni, Y.-C. Hou, J. Chem. Eng. Data 42, 971 (1997). https://doi.org/10.1021/je960351m
132. R.G. Ross, P. Andersson, Mol. Cryst. Liq. Cryst. 78, 35 (1981). https://doi.org/10.1080/00268948108082145
133. I.G. Gurevich, K.B. Gisina, V.K. Shitnikov, B.I. Tumanov, Inzh.-Fiz. Zh 43, 623 (1982).
134. M.J. Assael, J.P.M. Trusler, T.F. Tsolakis, Thermophysical Properties of Fluids. An Introduction to Their Prediction (Imperial College Press. World Scientific, London, U.K., 1996)
135. E. Tiesinga, P.J. Mohr, D.B. Newell, B.N. Taylor, J. Phys. Chem. Ref. Data 50, 033105 (2021). https://doi.org/10.1063/5.0064853

136. G.A. Olchowy, J.V. Sengers, Phys. Rev. Lett. 61, 15 (1988). https://doi.org/10.1103/PhysRevLett.61.15
137. R. Mostert, H.R. van den Berg, P.S. van der Gulik, J.V. Sengers, J. Chem. Phys. 92, 5454 (1990). https://doi.org/10.1063/1.458523
138. R.A. Perkins, H.M. Roder, D.G. Friend, C.A. Nieto de Castro, Physica A 173, 332 (1991). https://doi.org/10.1016/0378-4371(91)90368-M
139. P.T. Boggs, R.H. Byrd, J.E. Rogers, R.B. Schnabel, (ODRPACK, Software for Orthogonal Distance Regression, NISTIR 4834, v2.013 National Institute of Standards and Technology, Gaithersburg, MD, 1992),
140. G.A. Olchowy, J.V. Sengers, Int. J. Thermophys. 10, 417 (1989). https://doi.org/10.1007/BF01133538
141. R.A. Perkins, J.V. Sengers, I.M. Abdulagatov, M.L. Huber, Int. J. Thermophys. 34, 191 (2013). https://doi.org/10.1007/s10765-013-1409-z
142. C.H. Klute, W.D. Walters, J. Am. Chem. Soc. 68, 506 (1946). https://doi.org/10.1021/ja01207a045